Estuaries and Coasts (2025) 48:60
https://doi.org/10.1007/s12237-025-01484-6

Quantifying the Relative Importance of Sand Deposition and Dune Grasses to Carbon Storage in US Central Atlantic Coast Dunes

Katya R. Jay[1,2] · Sally D. Hacker[1] · Cedric J. Hagen[3,4] · John Stepanek[1] · Laura J. Moore[5] · Peter Ruggiero[3]

Received: 13 December 2023 / Revised: 19 December 2024 / Accepted: 7 January 2025 / Published online: 12 February 2025

Abstract

Coastal ecosystems such as mangroves, salt marshes, and seagrasses sequester large amounts of carbon per unit area due to their high productivity and sediment accumulation rates. However, only a handful of studies have examined carbon sequestration in coastal dunes, which are shaped by biophysical feedback between aeolian sediment transport and burial-tolerant vegetation. The goal of this study was to measure carbon storage and identify the factors that influence its variability along the foredunes of the US Outer Banks barrier islands of North Carolina. Specifically, differences in carbon stocks (above- and belowground biomass and sand), dune grass abundance, and sand supply were measured among islands, cross-shore dune profile locations, and dune grass species. Carbon varied among aboveground grass biomass (0.1 ± 0.1 kg C m^{-2}), belowground grass biomass (1.1 ± 1.6 kg C m^{-3}), and sand (0.9 ± 0.6 kg C m^{-3}), with the largest amount in belowground grass stocks. Aboveground grass carbon stocks were comparable to those in eelgrass beds and salt marshes on a per-area basis, while sediment carbon values in our study system were lower than those in other coastal systems, including other dune locations. Additionally, sand carbon density was positively related to patterns in dune sand supply and grass abundance, reflecting a self-reinforcing vegetation-sediment feedback at both high and low sand accumulation rates.

Keywords Carbon stocks · Coastal dunes · Ecosystem services · Beach and dune morphology · *Ammophila breviligulata* · *Uniola paniculata*

Introduction

As global atmospheric carbon dioxide concentrations increase due to human activities, carbon sequestration (i.e., the process of capturing and storing atmospheric carbon dioxide) by ecosystems has become an increasingly valuable service in mitigating climate change (Sarmiento & Gruber, 2002; Chmura et al., 2003; Potter, 2003; Luyssaert et al., 2008; Reay et al., 2008; Intergovernmental Panel on Climate Change, 2014; Howard et al., 2017). Most research on carbon sequestration has focused on open ocean and terrestrial ecosystems, with fewer studies in coastal ecosystems despite their role in global carbon cycling, carbon budgets, and climate regulation (Nellemann et al., 2009; Donato et al., 2011; Mcleod et al., 2011; Beaumont et al., 2014; Howard et al., 2017; Macreadie et al., 2019). The majority of coastal carbon sequestration measurements have been made in mangroves, seagrass beds, and salt marshes (Chmura et al., 2003; Steven Bouillon et al., 2008; Duarte et al., 2010; Kennedy et al., 2010; Breithaupt et al., 2012; Hopkinson et al., 2012;

Communicated by Richard Fulford

✉ Katya R. Jay
katya.jay@colorado.edu

[1] Department of Integrative Biology, Oregon State University, 2403 Cordley Hall, Corvallis, OR 97331, USA

[2] Present Address: Cooperative Institute for Research in Environmental Sciences, University of Colorado, Boulder, 4001 Discovery Drive, Boulder, CO 80303, USA

[3] College of Earth, Ocean, and Atmospheric Sciences, Oregon State University, 104 CEOAS Administration Building, Corvallis, OR 97330, USA

[4] Department of Geosciences, Princeton University, Princeton, NJ 08544, USA

[5] Department of Earth, Marine and Environmental Sciences, University of North Carolina at Chapel Hill, 104 South RoadChapel Hill, Mitchell Hall, NC 27559, USA

Greiner et al., 2013), where rates of carbon sequestration are relatively high, averaging 1380–2260 kg C ha^{-1} $year^{-1}$ compared to 40–51 kg C ha^{-1} $year^{-1}$ in temperate, tropical, and boreal forests and 540 kg C ha^{-1} $year^{-1}$ in grasslands (Conant et al., 2001; M. B. Jones & Donnelly, 2004; R. Lal, 2005; Mcleod et al., 2011; Duarte, 2017; Rattan Lal et al., 2018). Although the rates of carbon sequestration in coastal habitats are often high per unit area, their overall global carbon storage is modest given their smaller geographic area compared to that of forest and open ocean ecosystems (Cao & Woodward, 1998; Howard et al., 2017; Mcleod et al., 2011).

Carbon sequestration rates in coastal ecosystems are largely a product of high vegetation productivity and high sediment and marine carbon imported from coastal waters (Mcleod et al., 2011), often keeping pace with sea level changes (Chmura et al., 2003). Research in salt marshes, mangroves, and seagrass meadows shows that the origin of carbon stocks can vary from locally produced to imported depending on local biotic characteristics and environmental factors such as tidal range and sediment transport rates (Bouillon et al., 2003; Kristensen et al., 2008; Middelburg et al., 1997).

One coastal ecosystem that has received relatively little attention for its potential to store carbon is coastal dunes, a widespread ecosystem that occurs worldwide (recent estimates indicate that 31% of ice-free coastlines are sandy beaches and dunes; Luijendijk et al., 2018). Although ecosystem services such as coastal protection and recreation have been widely recognized as important in dunes (Barbier et al., 2011), less is known about their ability to sequester carbon, even though they have vegetation densities and sedimentation rates similar to marshes (Drius et al., 2016; Jones et al., 2008; Olff et al., 1993). Where carbon sequestration has been measured in coastal dunes (Table 1), the values are lower than those in other coastal ecosystems. From the limited number of observations available, average sediment carbon sequestration rates for dunes range from 56 to 730 kg C ha^{-1} $year^{-1}$ (Table 1). These values are low compared to mangroves, salt marshes, and eelgrass meadows, which have values ranging from 1380 to 2260 kg C ha^{-1} $year^{-1}$ (Mcleod et al., 2011). However, given the geographic extent of sandy beaches, dunes (Luijendijk et al., 2018) may have the potential to capture and store substantial carbon globally. In addition, most measurements in dunes have not considered how carbon sequestration varies with depth, dune cross-shore profile location, or dune plant community (Table 1; Barbier et al., 2011; Kristensen et al., 2008; Middleton & McKee, 2001).

Foredunes, or the seaward-most dune ridge parallel to the ocean, are dynamic ecosystems shaped by sea level, wind and wave conditions, sediment supply, beach morphology, and vegetation (Bauer & Davidson-Arnott, 2002; Cohn et al., 2019; Duran & Moore, 2013; Hesp, 1989, 2002; Hesp & Walker, 2013; Jay et al., 2022a; Keijsers et al., 2016; Moore et al., 2016; Ruggiero et al., 2016; Sherman & Bauer, 1993; Short & Hesp, 1982; Zarnetske et al., 2015). Dunes form via biophysical interactions in which burial-tolerant vegetation, such as dune grasses, slows sand-laden wind, leading to sand deposition and subsequent plant growth; this process continues as a positive feedback between vegetation and sand accumulation, potentially leading to fully formed foredunes (Biel et al., 2019; Brown & Zinnert, 2018; Charbonneau et al., 2021; Hacker et al., 2012; Keijsers et al., 2015; Mullins et al., 2019; Zarnetske et al., 2012). Early research demonstrated relationships between dune shape and grass species (Godfrey & Godfrey, 1973; Van der Valk, 1975; Woodhouse et al., 1977), while more recent studies have shown that plant density, morphology, and belowground growth patterns all contribute to a range of different dune morphologies (P. Biel et al., 2019; Goldstein et al., 2017; Hacker et al., 2012, 2019; Hesp, 2002; Jay et al., 2022a, 2022b; Laporte-Fauret et al., 2021; Zarnetske et al., 2012).

The combination of physical and ecological factors that shape beach and dune morphology could play an important role in carbon sequestration. For example, vegetation density and biomass can influence standing carbon stocks and the amount of organic matter available for burial (Beaumont et al., 2014). In turn, the amount of sand deposited on the dune might dictate how much organic matter is buried. Marine-derived carbon contained in macroalgal wrack and beach sand may be an additional source of carbon for dunes (Barreiro et al., 2013; Dugan et al., 2011). Finally, at a larger scale, the physical processes that shape beaches and dunes—including dune scarping and erosion, storm overwash, aeolian sand transport, and inlet dynamics (for barrier systems)—may influence carbon sequestration, as these processes can rapidly bury or expose organic matter and vegetation following major depositional or erosional events (Rossi & Rabenhorst, 2019), such as those occurring during extreme storms (Macreadie et al., 2019).

In this study, we measure carbon storage (i.e., the amount of carbon stored in sand and vegetation) in foredunes along the Outer Banks of the US Central Atlantic coast, a ~ 300-km string of vegetated barrier islands—extending from the border between Virginia and North Carolina (NC) in the north to Cape Lookout, NC in the south—that are highly vulnerable to coastal erosion from sea-level rise and extreme storms (Hovenga et al., 2021; Paerl et al., 2019; Sallenger et al., 2012). This region has widespread dunes exhibiting dramatic variation in beach and dune morphology, sand supply, and vegetation abundance and composition, making it an ideal system for studying dune carbon sequestration (Goldstein et al., 2018; Hacker et al., 2019; Hovenga et al., 2019, 2021; Jay et al., 2022a; Kratzmann et al., 2017; Stockdon et al., 2007; Van der Valk, 1975). Sand supply and beach

Table 1 Summary of studies in which percent soil organic carbon (SOC), organic carbon stocks (tonnes ha^{-1}), and carbon sequestration rates (kg ha^{-1} $year^{-1}$) were measured in coastal dunes

Reference	Location	Sampling depth (cm)	SOC content (%)	Org. carbon stocks (t ha^{-1})	Carbon sequestration rate (kg ha^{-1} $year^{-1}$)
Tackett and Craft (2010)	Sapelo Island, Georgia, USA	0–30	0.08 ± 0.01 (top 10 cm); 0.06 ± 0.01 (10–30 cm)	2.5	
Drius et al. (2016)	North and Central Adriatic, Italy	0–15	0.13 ± 0.05 (embryo dunes); 0.15 ± 0.12 (mobile dunes); 0.18 ± 0.07 (fixed dunes); 2.84 ± 2.56 (wooded dunes)	3.1 ± 1.3 (embryo dunes); 3.1 ± 1.7 (mobile dunes); 4.1 ± 1.4 (fixed dunes); 31 ± 19.7 (wooded dunes)	57.2 ± 22.8 (embryo dunes); 55.7 ± 31 (mobile dunes); 74.9 ± 25.6 (fixed dunes); 563.5 ± 358.3 (wooded dunes)
Jones et al. (2008)	Atlantic UK dunes, North Wales	0–15			582 ± 262 (dry dunes); 730 ± 221 (wet dunes)
Beaumont et al. (2014)	Atlantic UK dunes (Wales, Scotland, England, North Ireland)	0–15	0.33 ± 0.22 (mobile dunes); 1.84 ± 1.71 (fixed dunes); 4.38 ± 3.32 (dune slacks)		
Turner and Laliberté (2015)	Jurien Bay chronosequence, SW Australia	0–100		Ranges from 29.2 to 177.2 depending on age	
Schaub et al. (2019)	SW Baltic Sea, NE Germany	0–1.5	0.03		
Chen et al. (2015)	Cooloola Dunes, South Queensland, Australia	0–30	Ranges from 0.03 (bare sand) to 1.44 (vine forest scrub) *(total C, not org. C)	Ranges from 0–60 depending on age * (total C, not org. C)	

Values are based on sand carbon measurements and do not include dune vegetation

geomorphology vary widely along the NC coast, where some sites have wider beaches with gently sloping dunes, while others have narrower, steeper beaches associated with taller, narrower dunes. From 1997 to 2016, the majority of beaches along the southern Outer Banks (from Shackleford Banks, SHB, to North Core Banks (NCB) have eroded, with negative multidecadal shoreline change rates (SCR; measured as average annual change in shoreline position), while beaches from Ocracoke Island northward have prograded (Hovenga et al., 2021; Jay et al., 2022a). Foredune height across the region increased by 0.01–0.02 m year^{-1} on average over this period, while foredune toe position retreated landward (see Hovenga et al., 2021 for details).

Two native kinds of grass dominate Central Atlantic barrier islands: *Uniola paniculata*, a drought-tolerant warm-season grass extending from Virginia to Florida (Seneca, 1969), and *Ammophila breviligulata*, a temperate cool-season grass extending from NC to Canada (Goldstein et al., 2018; Hacker et al., 2019; Jay et al., 2022a). The two species overlap on the Outer Banks, where *A. breviligulata* creates more continuous, linear dunes compared to the steeper, more hummocky dunes of *U. paniculata* (Woodhouse et al., 1977). Two less abundant grasses, *Panicum amarum* and *Spartina patens*, are similar to *U. paniculata* in their distributions (Hacker et al., 2019). A study examining the functional morphology of all four grass species found that *A. breviligulata* was correlated with higher sand accretion, likely due to its dense, clumped growth form, while *U. paniculata* was associated with less sand accretion and fewer, larger, more evenly spaced shoots (Hacker et al., 2019). Thus, it may be that dunes vary in their ability to sequester carbon because of differences in grass biomass, growth form, and sand capture ability.

We measured how the carbon stored in dune vegetation and sand varies across spatial scales, including depth, dune cross-shore profile location, and barrier island location along a 225-km stretch of the Outer Banks barrier islands (Fig. 1A). We ask the following questions: (1) Does the amount of carbon in dunes vary with core depth, carbon stock type, island, and/or foredune profile location, and if so, how? and (2) If carbon storage varies, what geomorphological and ecological factors might explain this variability?

Methods

Field Sample and Data Collection

This study was conducted on the foredunes along 225 km of the NC Outer Banks from Bodie Island (BOD) in the north to South Core Banks (SCB) in the south (Fig. 1A; Table S1). This stretch of sandy barrier islands varies spatially in vegetation species and density (Hacker et al., 2019; Jay et al., 2022a, 2022b), beach geomorphology and shoreline orientation (Hovenga et al., 2019, 2021; Jay et al., 2022a, 2022b), and wave energy and underlying stratigraphy (Lazarus & Murray, 2011). Apart from hurricanes, which occur in the summer and fall, and nor'easters, which occur in the winter and spring, the region experiences a moderately energetic seasonal wind and wave climate (including average annual significant wave heights of ~ 1.2 m and wind speeds of ~ 6.8 m s^{-1}; Bryant et al., 2016). The Outer Banks region also exhibits significant alongshore variability in beach geomorphology and shoreline erosion (Hovenga et al., 2021). Foredune height and beach width can range from 1.5 to 5.5 m and ~ 30 to 55 m, respectively, along the southern extent of the region (including SCB and NCB; Hovenga et al., 2021). Foredune heights ranging from 3 to 11 m are typical father north (from Cape Hatteras northward; Woolard & Colby, 2002).

From 2017 to 2019, we surveyed vegetation communities and topography annually at 112 transects that ranged from 0.4 to 20.4 km apart (most were 1–5 km apart), depending on the island and beach access (see Hacker et al., 2019; Hovenga et al., 2019, 2021; Jay et al., 2022a, 2022b). Transects were shore-perpendicular, extending from mean lower low water (MLLW) through the dune toe (the seaward-most dune extent, marked by the topographic inflection point between the backshore and the foredune, and often also denoted by the vegetation line), crest (the highest point of foredune elevation), and heel (the lowest point on the landward side of the foredune) (see Fig. 1B). In June 2019, we resurveyed a subset of these transects ($n = 11$) for vegetation and topography and collected sediment cores and dune grasses at the toe, crest, and heel of the foredune for carbon measurements (see Table S1; Fig. 2 for transect and core collection locations). We selected this subset of transects to capture spatial variability in dominant grass species and sand supply across the five islands and the dune profile. For two of the three SCB transects (SCB_6 and SCB_9), the morphology of the foredune was substantially altered due to erosion from Hurricane Florence, which occurred nine months (September 2018) before our collections (Fig. 2). This erosion resulted in the removal of the toe and crest foredune profile locations from the original 2017/2018 transects (Fig. 2). The loss of the toe and crest profile locations was unknown to us at the time of sampling, so instead of coring at these profile locations, we collected all three cores at the heel location prior to September 2018 (see Fig. 2). Once the data were processed, we determined that topographic and vegetation data corroborated that these samples were more characteristic of the heel profile location than the toe or crest locations. Thus, for transects SCB_6 and SCB_9, we decided to classify all the cores and associated vegetation as "heel" samples in our data analysis and statistics.

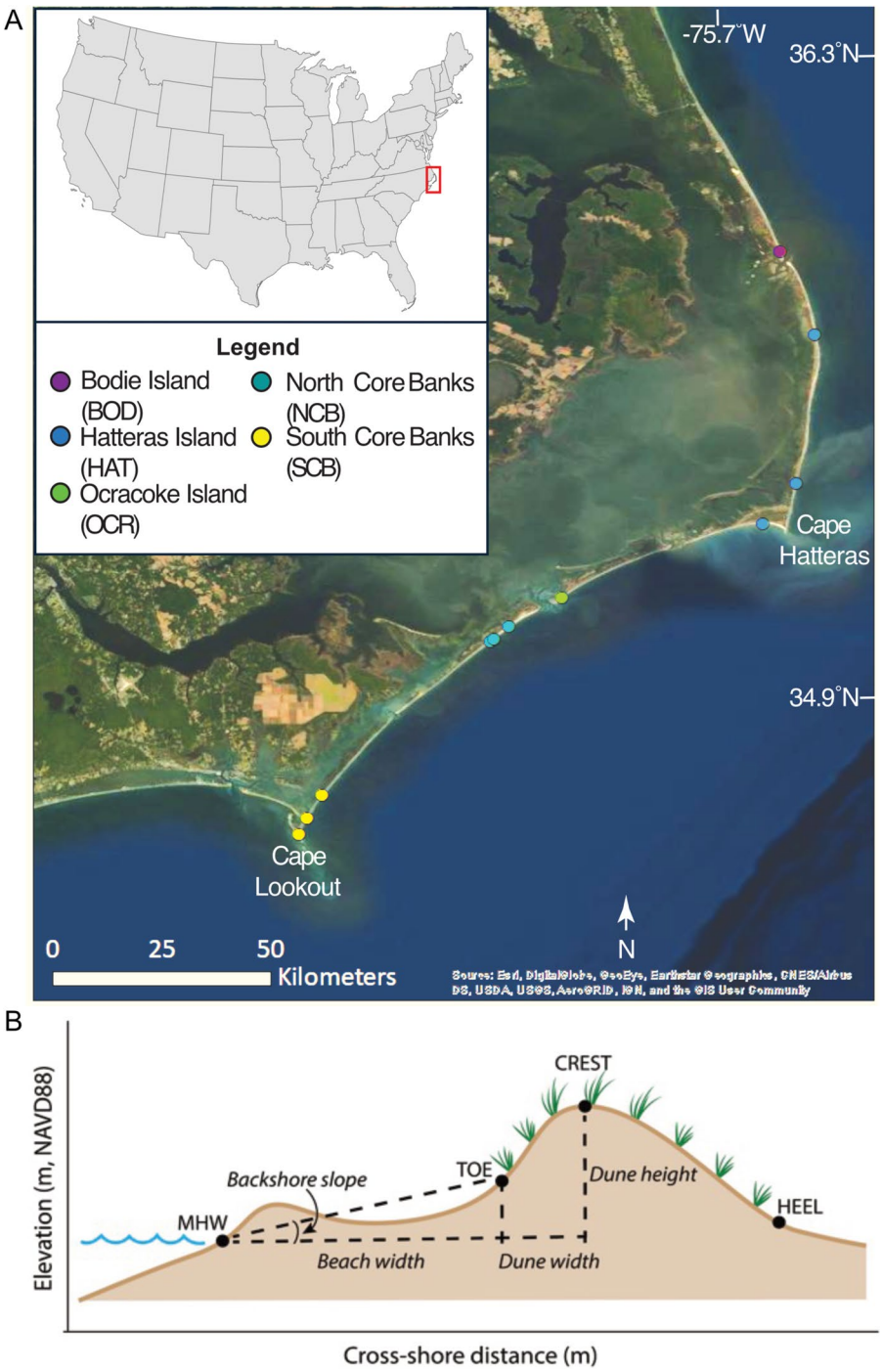

Fig. 1 **A** Map of transect and sediment carbon core sampling locations (see Table S1 for latitude and longitude) for the foredunes of the Outer Banks barrier islands, North Carolina, USA. **B** Beach and dune morphology parameters were calculated using data from real-time kinematic GPS surveys and following the methods of Mull and Ruggiero (2014). Mean high water (MHW) was extracted using the 0.4-m MHW contour (NAVD88). Foredune morphology measurements included the position and elevation of the foredune toe (the seaward extent of the foredune), the foredune crest (the highest point on the foredune), and the foredune heel (the landward extent of the foredune, determined by an elevation minimum). Foredune height and toe elevation were calculated as the differences between MHW and the foredune crest and toe elevations, respectively. Foredune width was calculated as one-half dune width (the horizontal distance between the foredune toe and crest) to capture changes in the width of the foredune face. The backshore slope was calculated as the slope between MHW and the dune toe. Beach width was calculated as the horizontal distance between MHW and the foredune toe. Figure adapted from Jay et al., (2022a, 2022b)

Along each of the 11 transects, vegetation surveys involved counting shoots of each grass species in 0.25 m^2 quadrats every 5 m using the methods in Hacker et al. (2019) and Jay et al. (2022a). Sediment cores (1-m depth) were collected at the toe, crest, and heel (three cores/transect), roughly 1 m away (but at the same elevation) from the transect to avoid disruption (Table S1; Fig. 2). At the core location, shoot densities of all grass species in a 0.25-m^2 quadrat were also counted, and individual plants (all shoots attached to one rhizome) of each species were collected. The topography of the transect and elevation of each quadrat and sediment core location were measured using a Network Real Time Kinematic (RTK) Differential Global Positioning System (R7 unit, Trimble, Sunnyvale, CA, USA) (Fig. 2).

Sediment core collection involved driving a 10-cm diameter PVC pipe into the toe, crest, and heel of the foredune using a sledgehammer and custom "core head" placed over the top of the core tube and inserting a test plug within the

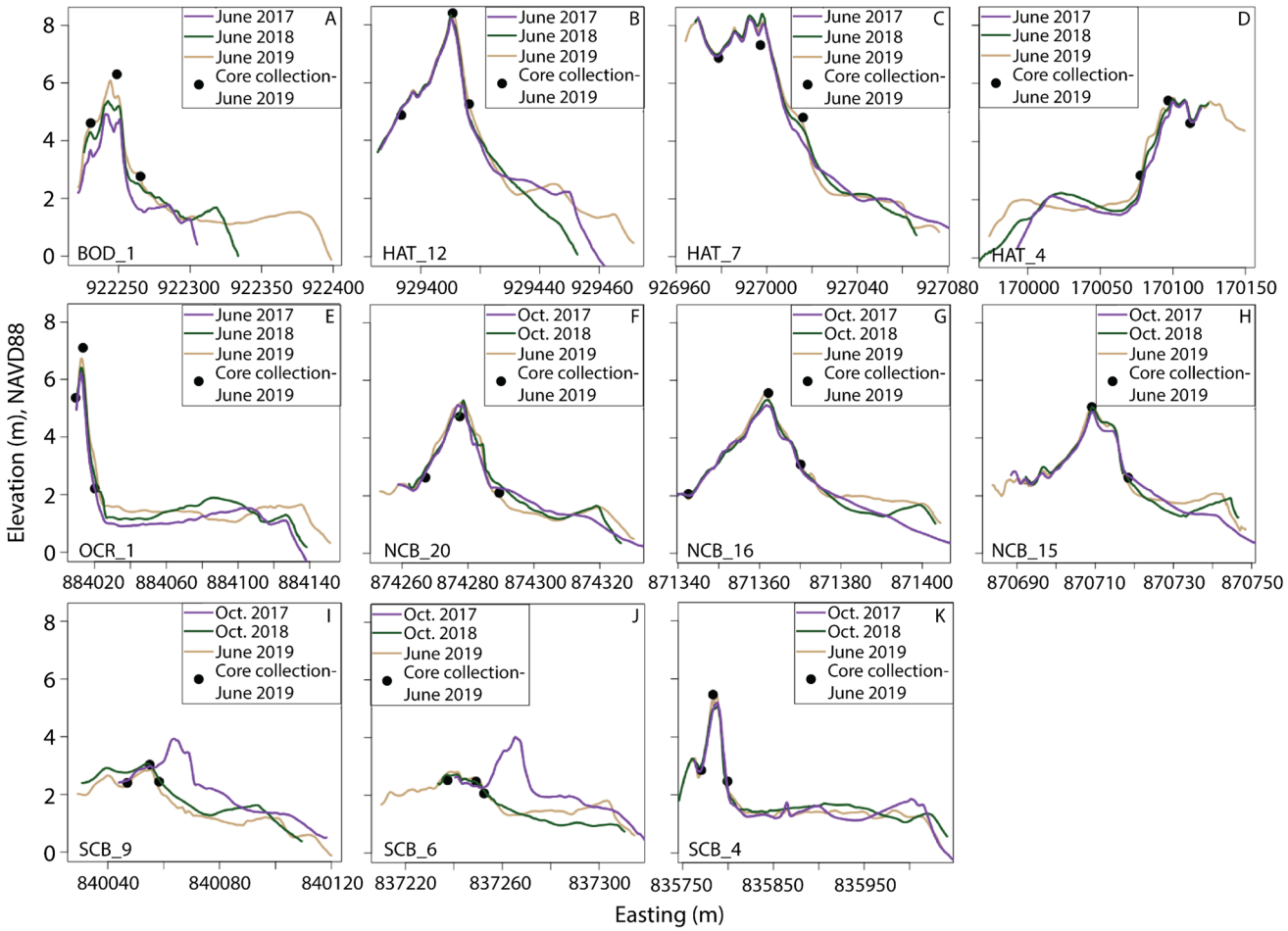

Fig. 2 Dune elevation profile plots from 2017 to 2019 for each transect surveyed on the Outer Banks barrier islands, North Carolina, USA, arranged from north to south (see Fig. 1A; Table S1 for profile locations and abbreviations). Colored lines represent the elevations from each year, while dots denote the locations where the cores were collected. All plots share the same *y*-axis scale. Note that the *x*-axis for HAT_4 is in northing (m) rather than easting due to the orientation of the transect

tube to prevent sediment loss upon removal (Fig. S1). Due to the difficulty of extruding a 1-m-long core of sand, two 0.5 m core tubes, one for the top 0.5 m and one for the bottom 0.5 m, were used for each core collection. The first tube was pounded into the top half of the 1 m core depth and dug out with a shovel, and the second tube was then inserted in the same location without disturbing the sediment to collect the remaining 0.5 m core. We extracted the sand and belowground plant material from the core in alternating depth intervals using a custom-built sediment extruder that slowly extruded sediment in 2-cm increments for subsampling (see Figs. S2 and S3). We haphazardly subsampled roughly a quarter of each layer (~ 30 ml) of sand and belowground plant material and discarded the remainder of the sample. Samples were collected every 2-cm increment, and the samples in between those increments were discarded.

Core Sample Processing and Sand Carbon Density Measurements

To determine sand carbon content in our cores, we calculated sand carbon density (g C m^{-3} sand), which is a product of bulk density (g cm^{-3} sand) and percent carbon content (% C) of our core samples. The bulk density of the sand was estimated by measuring the wet and dry weight (dried at 60 °C for 24 h) of a subset of samples that were representative of foredune profile locations and sites to obtain their percent moisture content. Bulk density was then calculated for each sample as a weighted average between dry sand density and freshwater density based on the average percent moisture using the following equation: $Bulk\ density\ (g\ cm^{-3}) = Dry\ sand\ density \times (1 - moisture\ proportion) + Freshwater\ density \times Moisture\ proportion$. The remaining core samples were

also dried (60 °C for 24 h), and then the roots and rhizomes, any other plant matter, and shells were removed from all samples using a 2-mm sieve and each was weighed separately.

We then used a subset of the sieved sand samples to determine percent organic matter (using loss on ignition or LOI) and percent organic carbon content (via elemental analysis) at different core depths, profile locations, and transects across islands (see Table S2 for a list of core sample measurements). For each core, all samples in the top 40 cm, and every third sample from the remainder of the core, were used for organic matter measurements. In addition, three samples per core per profile location (totaling 9 samples/transect = 96 samples total) were used to measure the percent total organic carbon content. Organic carbon samples were chosen using their percent organic matter values to ensure that a wide range of carbon values were measured (i.e., the highest, median, and lowest values were included for each core).

The loss on ignition (LOI) technique (see Heiri et al., 2001) involved burning 2.000 ± 0.002 g of each dried sand sample at 550 °C for 4 h and reweighing it once cooled. Burning the samples at 550 °C allows organic matter to combust without dissociating CO_2 from carbonates in the sand (Dean, 1974). Percent LOI was determined using the proportion of mass lost relative to the starting mass. Total organic carbon content was measured via elemental analysis using an ECS 4010 CHNSO Analyzer at the Oregon State University Elemental Analysis Facility, Corvallis, USA. Prior to elemental analysis, dried sand samples were homogenized using a Spex Sigma Prep 8000D Mixer/Mill followed by acidification with 1 M HCl to remove carbonates. Percent total organic carbon was calculated from the mass of organic carbon out of the total sample mass.

After measuring the percent organic matter and percent organic carbon content (for a subset of samples), we then established a relationship between these two measurements that could be applied to all samples to derive their percent total organic carbon (% TOC). Specifically, we established two regression relationships between percent organic matter (% LOI) and percent total organic carbon (% TOC). The first regression analysis included all samples except those from transect SCB_9, which had a higher ratio of % LOI to % TOC than the other samples (% TOC = 0.310 * % LOI – 0.015, $R^2 = 0.66$, $p < 2.2E\text{-}16$; see Fig. S4A). The second relationship was established for transect SCB_9 samples alone (% TOC = 0.509 * % LOI – 0.016, $R^2 = 0.45$, $p = 0.049$; see Fig. S4B). Note that five samples had % TOC values equal to or greater than % LOI values and were excluded from the analyses. Finally, to calculate sand carbon density (kg C m^{-3}) for each sample, we multiplied bulk density estimates by % TOC (converted to a proportion) using the equation: $Sand\ carbon\ density\ (g\ C\ cm^{-3}) = Bulk\ density\ (g\ cm^{-3}) \times Proportion\ TOC$.

Dune Grass Sample Processing and Carbon Measurements

We estimated the aboveground and belowground dune grass carbon density for the two most abundant species (*U. paniculata* and *A. breviligulata*) at each transect. All belowground measurements from a given core were classified as either *U. paniculata* or *A. breviligulata* based on the dominant species present above each core. Carbon density was measured as the product of grass percent carbon multiplied by the average biomass of each species. Note that here we use the general convention of expressing aboveground grass carbon density in area units (kg C per m^2 area) and the belowground grass carbon density in volumetric units (kg C per m^3) but the two measurements can be directly compared given that they consider the same 1 m^2 dune area.

The organic carbon content of the grasses was obtained using the following methods. For the aboveground grass samples, we measured carbon content in the tissues of each grass species collected near each core. For the belowground grass samples, we measured the organic carbon content of the root and rhizome tissues obtained from the cores. For both sets of samples, grass tissues were first homogenized in a Spex Sigma Prep 8000D Mixer/Mill, and organic carbon content was measured via elemental analysis using an Elementar Vario Macro Cube at the Oregon State University Soil Health Laboratory, Corvallis, OR, USA.

To estimate aboveground grass carbon density, we dried and weighed each dune grass shoot sample. We then calculated the aboveground grass biomass (g m^{-2}) for each species as the product of the average shoot weight and average shoot density (shoots/0.25 m^2 in the field from 2017 to 2019, converted to m^2) at each transect and profile location. Aboveground grass carbon density (kg C m^{-2}) was then calculated for each quadrat as the product of species-specific aboveground biomass and average species-specific percent organic carbon content.

To estimate belowground grass carbon density, we used three methods for different scales of measurement. The first method was used to estimate belowground grass carbon density with depth in the core. To do this, the belowground grass biomass sifted out of individual core samples was multiplied by the average belowground grass organic carbon content and converted to kg C m^{-3}. The second method involved extrapolating the proportion of belowground biomass sifted out of each core sample (i.e., belowground biomass per weight of sand) to the volume of the entire core. Belowground grass carbon density for each core was then calculated as the product of belowground biomass multiplied by the average belowground organic carbon content and converted to kg C m^{-3}. The third method was used to estimate spatial variability in belowground grass carbon density along each transect using aboveground biomass as

a proxy. We calculated the ratio between aboveground (in quadrats directly above each core) and belowground grass carbon density for each core (based on the second method above) and applied that ratio to the remaining quadrats along each transect in order to obtain an estimate of the variability in belowground grass carbon density in areas where we were unable to measure it directly.

Beach and Foredune Morphometrics, Shoreline Change Rate, and Sand Supply

To assess potential drivers of variation in dune carbon density, we obtained beach and foredune morphometrics and SCRs at each transect from Jay et al., (2022a, 2022b). Morphometric measurements included beach width (distance from mean high water, or MHW, to foredune toe), backshore slope (slope from MHW to foredune toe), foredune height (vertical distance from MHW to dune crest elevation), foredune width (horizontal distance between foredune toe and crest), and foredune aspect ratio (foredune height divided by width). We extracted MHW using the 0.4-m contour referenced to the North American Vertical Datum 1988 (NAVD88; see Hovenga et al., 2021). To estimate vertical sand supply or loss at each core collection site, we calculated sand deposition or erosion along the transects as the vertical change in the elevation (m; representing a net gain or loss of sand) of the foredune toe, crest, and heel for each year (locations of each feature were chosen in 2017, and the same cross-shore location was used in following years to assess vertical change from 2017 to 2019) and then calculated the total and annual sand deposition (or erosion) between years.

Statistical Analyses

We used R v.3.6.1 (R Development Core Team, 2019) for all statistical analyses. Residual and normal quantile plots were used to assess whether response variables conformed to the assumptions of the analyses, and natural log transformations of response variables were appled when necessary (see Table 2).

To assess spatial patterns of carbon density on Outer Banks foredunes, we used two-way ANOVAs and Tukey HSD post hoc tests. If significant interactions were found, we performed one-way ANOVAs and Tukey HSD post hoc tests to compare between levels of each factor (Underwood, 1997). We first conducted two-way ANOVAs separately for each transect to test for differences in sand carbon density and belowground grass carbon density among core depths and profile locations. Additional two-way ANOVAs were then run across all transects for (1) total carbon density by carbon stock type (aboveground and belowground grass and sand) and island, and (2) aboveground grass carbon density, belowground grass carbon density, and sand carbon density by island and dune profile location. All three cores from the two heavily eroded SCB transects (Fig. 2I, J) were categorized as dune heel sites in all analyses.

To investigate potential factors influencing variability in dune carbon density, we used multiple linear regression analyses to evaluate the relative importance of geomorphic and ecological factors associated with the response variables of aboveground grass carbon density, belowground grass carbon density, sand carbon density, and total carbon density (aboveground grass + belowground grass + sand). For the grass carbon density response variables, we tested for a relationship with explanatory metrics of annual sand deposition or erosion (2017–2019; calculated as the vertical change in elevation as described above), multidecadal SCR, beach width, backshore slope, foredune height, foredune width, and foredune aspect ratio. For sand carbon density, explanatory metrics included annual sand deposition to the dune (2017–2019), multidecadal SCR, grass biomass, grass tiller density, beach width, backshore slope, foredune height, foredune width, and foredune aspect ratio. Top models were selected from these linear regression analyses using sample size-corrected Akaike's Information Criterion (AIC_c). To determine the relative contribution of individual predictors in the top models, we used the R package "heplots" and the function "etasq" to calculate multivariate eta-squared (or R^2) (Fox et al., 2018).

To calculate the dune grass density values, the tiller density of all three species in quadrats (converted to m^2) from the 2019 surveys was summed and averaged for each transect and dune profile location. For the two eroded SCB sites, grass tiller density values from 2017 were used to represent the pre-hurricane vegetation community. To calculate the dune grass biomass values, the densities of each species from 2019 were multiplied by their mean tiller weights and summed and then averaged for each transect and profile location.

Results

Patterns in Geomorphology, Sand Supply, and Dune Grasses

Beach and foredune morphology, SCRs, sand supply, and dune grass metrics varied across the study region (Fig. 3; Jay et al., 2022a). At most transects, multidecadal SCR values ranged from either slightly positive to negative, indicating mild accretion or erosion at these locations, but exceptions include the BOD_1 transect (the only BOD transect; Table S1), which had > 10 m $year^{-1}$ of beach erosion, and HAT_4, OCR_1, and SCB_4 with

Table 2 Top model results (ΔAIC < 2) from multiple regression analyses of the response variables: sand carbon density (kg C m^{-3}), aboveground (AG) grass carbon density (kg C m^{-2}), and total carbon density (AG grass, belowground grass (BG), and sand combined) as a function of the explanatory variables of sand supply, beach and foredune morphometrics, and dune grass biomass and density (see Fig. 3) at the core level

Response variable	Model	Model results
Sand carbon density	[ln(Sand C)] = −1.91 [Sand dep rate]*** – 15.82 [Backshore slope]*** + 0.005 [Grass density]^ + 0.27*	AIC_c = 30.21; ΔAIC = 0; *df* = 29; Adj. R^2 = 0.70 Variance explained: sand dep rate = 0.50, backshore slope = 0.26, grass density = 0.04
	[ln(Sand C)] = −1.79 [sand dep rate]*** − 15.85 [backshore slope]*** + 0.001 [grass biomass]^ + 0.26	AIC_c = 30.70; ΔAIC = 0.49; *df* = 29; Adj. R^2 = 0.70 Variance explained: sand dep rate = 0.46, backshore slope = 0.25, grass biomass = 0.03
	[ln(Sand C)] = −1.81 [sand dep rate]*** − 14.76 [backshore slope]*** + 0.37**	AIC_c = 31.56; ΔAIC = 1.35; *df* = 30; Adj. R^2 = 0.67 Variance explained: sand dep rate = 0.47, backshore slope = 0.23
AG grass carbon density	[AG grass C] = 0.01 [Foredune height]^ + 0.02	AIC_c = −91.97; ΔAIC = 0; *df* = 31; Adj. R^2 = 0.06 Variance explained: foredune height = 0.09
	[AG grass C] = 0.01 [foredune height]^ − 0.003 [SCR] + 0.02	AIC_c = −91.36; ΔAIC = 0.61; *df* = 30; Adj. R^2 = 0.09 Variance explained: foredune height = 0.10, SCR = 0.05
	[AG grass C] = 0.01[Foredune height]^ + 0.04[Sand dep rate] + 0.02	AIC_c = −90.45; ΔAIC = 1.52; *df* = 30; Adj. R^2 = 0.06 Variance explained: foredune height = 0.07, sand dep rate = 0.03
	[AG grass C] = 0.01 [foredune height]^ − 0.0002 [beach width] + 0.03	AIC_c = −90.26; ΔAIC = 1.71; *df* = 30; Adj. R^2 = 0.05 Variance explained: foredune height = 0.09, beach width = 0.02
Total carbon density (AG + BG + sand)	[ln(Total C)] = 0.07 [SCR]* + 0.55***	AIC_c = 74.59; ΔAIC = 0; *df* = 31; Adj. R^2 = 0.17 Variance explained: SCR = 0.19
	[ln(Total C)] = −1.20 [sand dep rate]* − 12.90 [backshore slope]* + 1.34 [foredune aspect ratio] + 0.63	AIC_c = 75.65; ΔAIC = 1.06; *df* = 30; Adj. R^2 = 0.22 Variance explained: sand dep rate = 0.14, backshore slope = 0.11, foredune aspect ratio = 0.06
	[ln(Total C)] = −1.18 [sand dep rate]* − 11.92 [backshore slope]^ + 1.06***	AIC_c = 75.69; ΔAIC = 1.10; *df* = 30; Adj. R^2 = 0.18 Variance explained: sand dep rate = 0.13, backshore slope = 0.10
	[ln(Total C)] = 0.06 [SCR]* + 6.10 [foredune aspect ratio] + 0.23	AIC_c = 75.97; ΔAIC = 1.38; *df* = 30; Adj. R^2 = 0.17 Variance explained: SCR = 0.18, foredune aspect ratio = 0.03
	[ln(Total C)] = 0.05 [SCR]^ − 0.61 [sand dep rate] + 0.63***	AIC_c = 76.10; ΔAIC = 1.51; *df* = 30; Adj. R^2 = 0.17 Variance explained: SCR = 0.09, sand dep rate = 0.03
	[ln(Total C)] = 0.06 [SCR]* − 6.10 [backshore slope] + 0.74***	AIC_c = 76.30; ΔAIC = 1.71; *df* = 30; Adj. R^2 = 0.16 Variance explained: SCR = 0.12, backshore slope = 0.02

Explanatory variables included in the models were uncorrelated with Pearson correlation coefficient < |0.6|. Significance codes for explanatory variables are as follows: ***$p < 0.001$; **$p < 0.01$; *$p < 0.05$, ^$p < 0.1$. Explanatory variables with significant p values are in bold. Response variable transformations were applied following Shapiro–Wilk tests for normality and residual analysis

4–10 m $year^{-1}$ of beach progradation (Fig. 3A). Most transects also had relatively narrow beaches (50 m or less) and steep backshore slopes (> 0.02; Fig. 3B, C). Two of the transects with positive multidecadal SCR values (SCB_4 and OCR_1) also had wide beaches (nearly 175 m wide) and shallow backshore slopes (Fig. 3A–C). Foredune height generally decreased from north to south, with the tallest dunes (> 8 m) occurring on Hatteras Island (HAT) and the shortest dunes (~ 4 m) occurring on SCB (Fig. 3D). Foredune width varied from ~ 10 to 30 m and did not follow a trend that was dependent on the island (Fig. 3E).

Sand deposition (or erosion) rate at the core locations (calculated from 2017 to 2019) tended to be unrelated (based on visual comparison) to multidecadal SCR (calculated from 1997 to 2016), beach width, or backshore slope (Fig. 3F). For example, the BOD transect located on a highly eroding beach had the greatest sand deposition across all profile locations (~ 0.75–1.0 m $year^{-1}$), followed by two HAT transects (HAT_12 and HAT_7), which had slightly negative SCRs. Moreover, transects with the most positive SCRs and widest beaches had patterns of sand deposition (or erosion) across the foredune

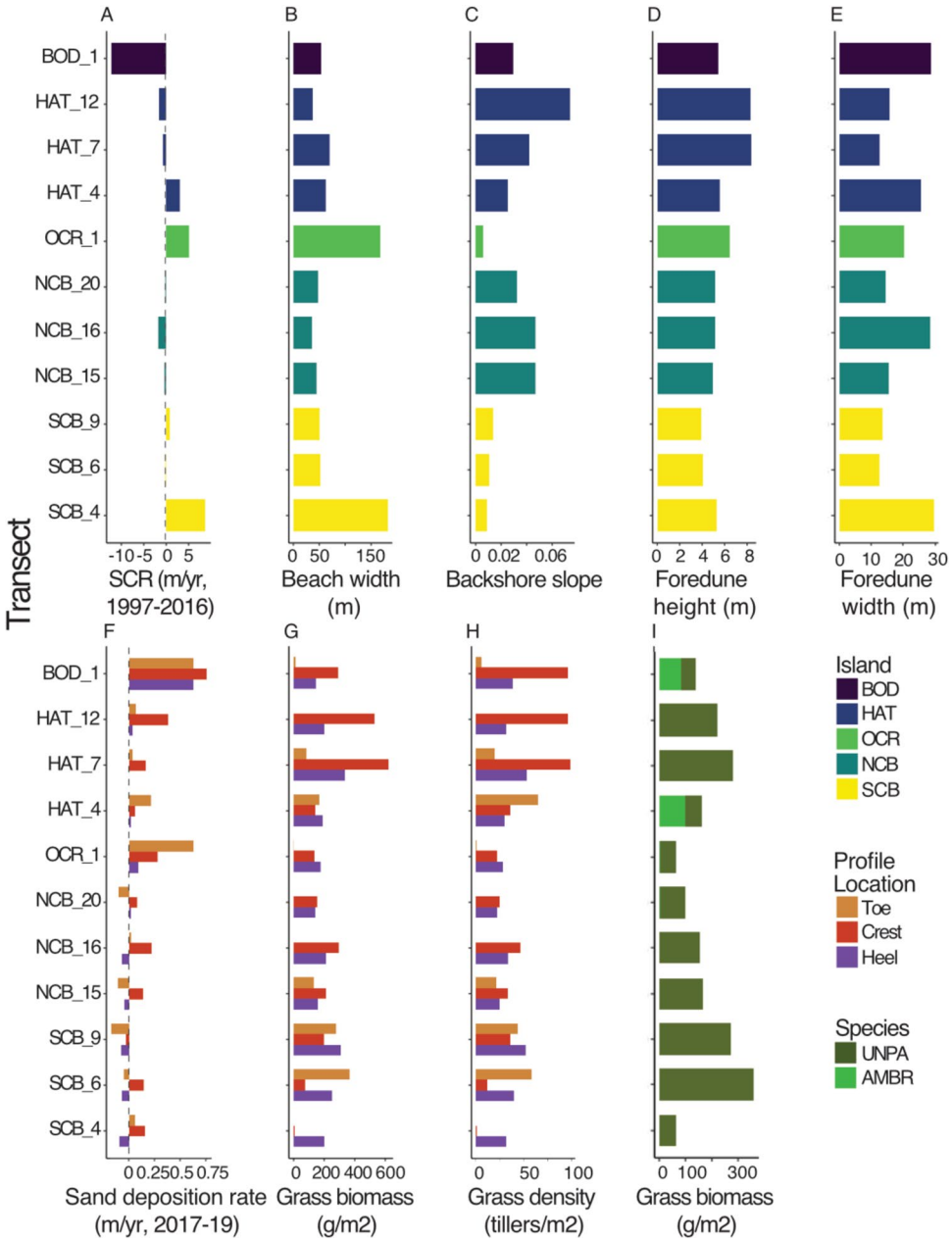

Fig. 3 Sand supply, beach morphology, and dune grass metrics for the foredunes of the Outer Banks barrier islands, North Carolina, USA, organized by transect from north to south (see Fig. 1A; Table S1 for island and transect abbreviations and locations). **A** Multidecadal shoreline change rate (SCR) from 1997 to 2016 (southern Outer Banks transects) and from 1997 to 2010 (northern Outer Banks transects) (m year^{-1}). **B** Beach width (m). **C** Backshore slope. **D** Foredune height (m). **E** Foredune width (m). **F** Annual sand deposition rate at the dune toe, crest, and heel from 2017 to 2019 (m year^{-1}). Note: All deposition values from SCB_6 and SCB_9 (across the toe, crest, and heel sites) were treated as heel sites in our analyses. **G** Mean combined grass biomass at the toe, crest, and heel of the dune in 2019 (g m^{-2}). **H** Mean combined grass density at the toe, crest, and heel of the dune in 2019 (tillers m^{-2}). **I** Mean combined grass biomass (2019, g m$^{-.2}$) of the dominant grasses, averaged across the dune profile and categorized by species: (*Uniola paniculata* (UNPA) and *Ammophila breviligulata* (AMBR))

that were similar to those of beaches with more neutral or slightly negative SCRs.

Grass species abundance (density and biomass) and distribution also varied across the study site and across foredune profile locations (Fig. 3G–I; Fig. S6; see Hacker et al., 2019 for detailed vegetation patterns). In general, *Uniola paniculata* was more widespread and had greater abundance than *A. breviligulata*, but this pattern also depended on the island and profile location. Specifically, the northern islands and the foredune toe locations generally had more *A. breviligulata* compared to the southern islands and foredune heel locations, which tended to have more *U. paniculata*.

Patterns of Sand and Belowground Grass Carbon Density with Core Depth

There was no consistent pattern in sand and belowground grass carbon metrics with core depth (Fig. S6; Table S3). Two-way ANOVAs between depth and profile location at each site showed that sand and belowground grass carbon metrics rarely differed by depth, though some profile location effects and depth-by-profile location interactions were observed (see Table S4 for details). A few notable depth patterns were seen at the heel of the dune: OCR_1, SCB_4, and HAT_4 had lower belowground grass and

sand carbon values at the top of the core, while NCB_20 had lower belowground grass and sand carbon values at the bottom of the core.

Patterns in Carbon Density Among Stock Types, Islands, and Foredune Profile Locations

The mean total carbon density (combining dune grasses and sand) across all stock types, islands, and foredune profile locations was 2.1 ± 1.8 kg C m^{-3} (mean ± SD) (Table S5). Belowground grass carbon density was the largest and most variable component of total carbon density (mean ± SD: 1.1 ± 1.6 kg C m^{-3}), followed by sand carbon density (0.9 ± 0.6 kg C m^{-3}) and aboveground grass carbon density (0.1 ± 0.1 kg C m^{-2}). A two-way ANOVA comparing carbon stock type and dune profile location showed a significant interaction between carbon stock type and profile location (Fig. 4; Table S6). Post hoc tests revealed that aboveground grass carbon density was significantly lower than both belowground grass and sand carbon density at the toe, crest, and heel (see Fig. 4). Additionally, belowground grass and sand carbon densities were not significantly different at the crest and heel (Table S6). The dune toe was an exception to this pattern, with higher sand carbon density than belowground grass carbon density (Fig. 4). Furthermore, the dune toe exhibited the lowest values for both aboveground and belowground grass carbon density, and

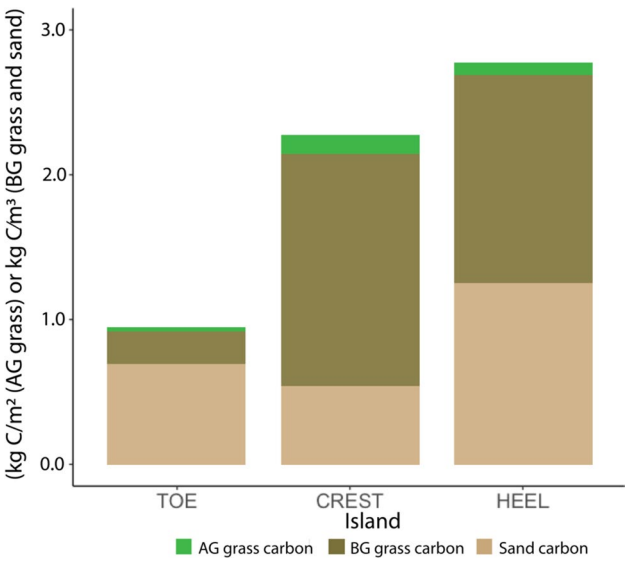

Fig. 4 Mean carbon density in aboveground (AG) grass (kg C m^{-2}), belowground (BG) grass (kg C m^{-3}), and sand (kg C m^{-3}) on the foredunes of the Outer Banks barrier islands, North Carolina, USA (see Fig. 1A; Table S1 for island abbreviations and locations). See Table S3 for mean (± SD) AG grass, BG grass, and sand carbon values separated by island and profile location, and Table S6 for statistics

both the toe and crest had lower values of sand carbon density than the heel. Total carbon stocks also varied by profile location, ranging from 1.0 ± 0.1 (toe; mean ± SE) to 2.8 ± 0.3 (heel) kg C m^{-2}.

The response variables of aboveground grass, belowground grass, and sand carbon density all showed variability among islands and profile locations, with significant island × profile location interactions (Fig. 5; Tables S5 and S7). For aboveground grass carbon density, the dune toe had lower values compared to the crest and heel (see Table S5), which did not differ, on all islands except BOD (toe = crest = heel) and HAT (crest > heel = toe) (Fig. 5A; Table S7). Within each profile location, aboveground grass carbon generally did not vary among islands, except at HAT and BOD, where dune crest carbon was higher than at NCB (HAT only) and SCB (both islands; Fig. 5A). Belowground grass carbon density exhibited similar patterns to aboveground grass carbon stocks: lower values at the dune toe compared to the crest and heel, which did not differ (Fig. 5B; Table S7). There were no differences in belowground grass carbon density among islands at the dune toe and heel, but values at the dune crest were significantly higher at OCR compared to other islands. Finally, sand carbon density varied among islands, with the southern Outer Bank islands (i.e., SCB and NCB) generally having higher values than the northern Outer Bank islands (i.e., BOD, HAT, and OCR; see Table S5 for values). However, this pattern depended on dune profile location (island × profile location interaction; Fig. 5C; Table S7). A landward gradient in sand carbon density was observed, with the toe and crest having lower values compared to the heel on all islands except BOD (no differences with profile location) and NCB (no differences between heel and toe). Additionally, on most islands, there were no differences in sand carbon density between the dune toe and crest. The only exception was NCB, where toe values were greater than crest values (Tables S5, S7).

Patterns in Carbon Stocks of Dominant Dune Grass Species

There were no differences in tissue carbon content between the two dominant grass species (mean ± SD; *U. paniculata* 46.88 ± 0.69% C, *A. breviligulata* 46.87 ± 0.74% C). Overall, dunes dominated by *U. paniculata* tended to have higher above and belowground carbon stocks compared to those dominated by *A. breviligulata* (Table S8). Note that BOD and HAT had the highest proportion of *A. breviligulata*, whereas SCB had no *A. breviligulata* (Fig. 3I; Table S8). Of the four islands where both species occurred, areas dominated by *U. paniculata* had similar or higher

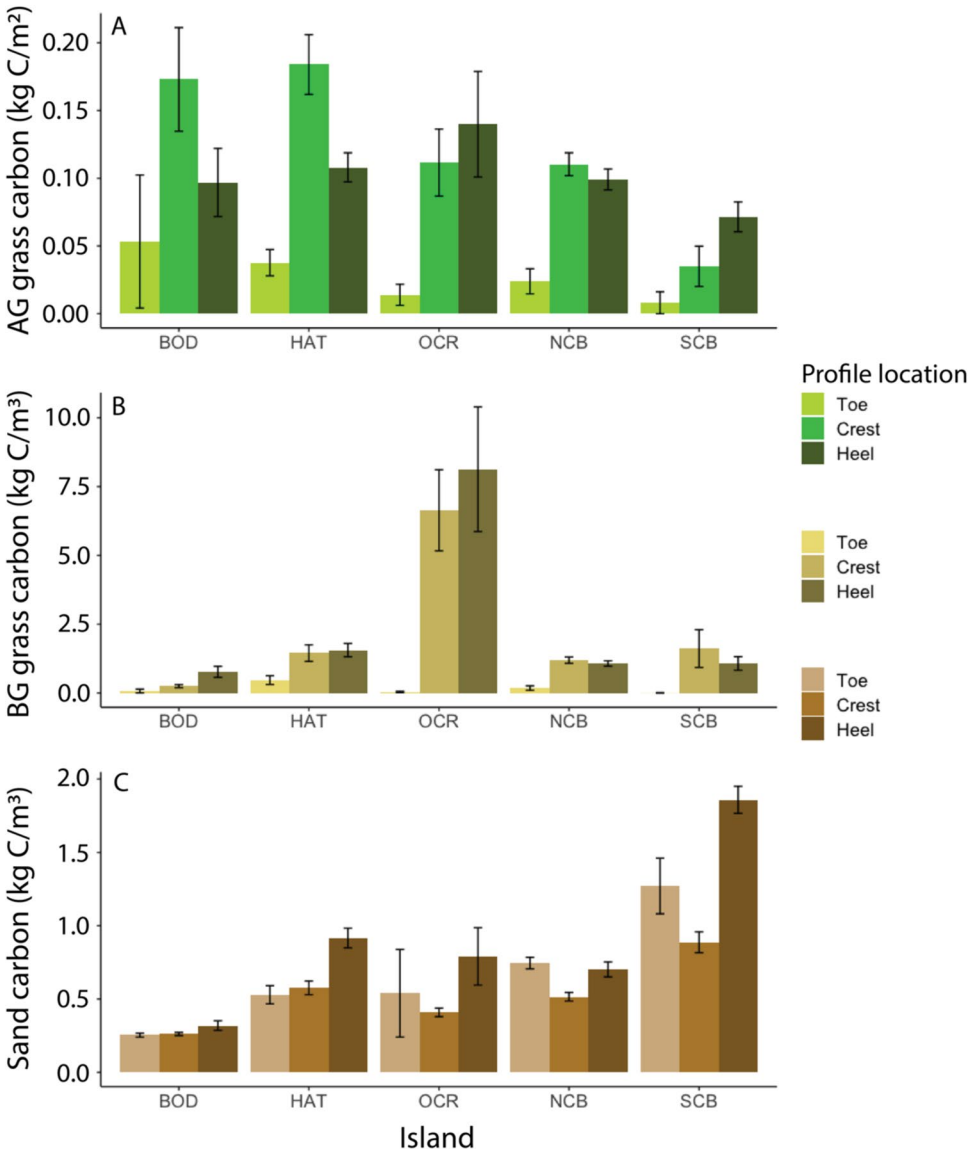

Fig. 5 Mean (±SE) **A** aboveground (AG) dune grass carbon density (kg C m^{-2}), **B** belowground (BG) dune grass carbon density (kg C m^{-3}), and **C** dune sand carbon (kg C m^{-3}) at three foredune profile locations (toe, crest, and heel) on the Outer Banks barrier islands, North Carolina, USA (see Fig. 1A; Table S1 for island abbreviations and locations). See Table S7 for statistics

sand carbon density than those dominated by *A. breviligulata*. However, this pattern coincides with variation in the occurrence of the two species across the dune profile (Table S8), with *U. paniculata* being dominant at the heel, where carbon density values were generally higher, and *A. breviligulata* occurring at the toe and crest, where carbon densities were lower (Figs. 2I and 4).

Factors Important to Carbon Stocks in Outer Banks Foredune Ecosystems

Our analyses revealed that patterns in sand carbon, aboveground grass carbon, and total carbon response variables were correlated with sand deposition to the dune, SCR, foredune height, and grass density and biomass (Table 2). First, mean sand carbon density was negatively correlated with sand supply metrics (annual 2017–2019 sand deposition rate at the core location and backshore slope, $p < 0.0001$ and $n = 33$ in both cases), while it was positively correlated with grass density and biomass (bordering on significant, $p = 0.06$ and $p = 0.08$, respectively, and $n = 33$ in both cases; Fig. 6; Table 2). In particular, the top model for sand carbon density indicated that the sand deposition rate at the core location explained the greatest proportion of variability (50%), followed by backshore slope (26%) and grass density (4%; Table 2). Second, the best-supported models for aboveground grass carbon stocks showed both positive (foredune height, $p = 0.09$, and sand deposition rate, $p = 0.33$; $n = 33$ for both) and negative (SCR, $p = 0.18$ and beach width, $p = 0.38$; $n = 33$ for both) correlations with aboveground carbon. However, only foredune height approached significance ($p = 0.09$, Table 2).

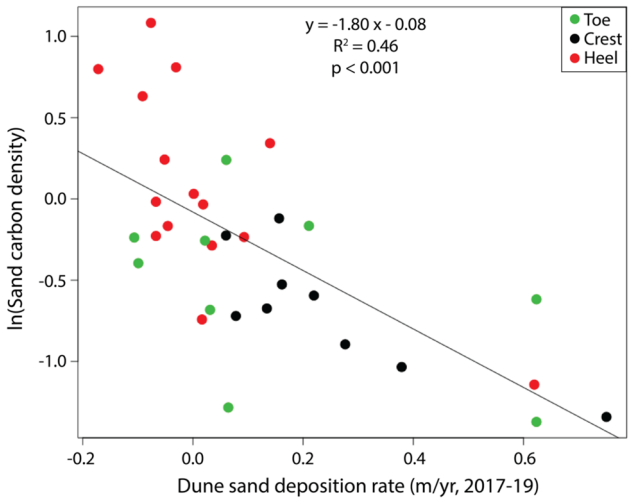

Fig. 6 Relationship between mean natural log (ln) sand carbon density (kg C m^{-3} at the core level) and annual sand deposition (or erosion) rate to the dune from 2017 to 2019 (m $year^{-1}$). Colors indicate cores collected at the toe, crest, and heel of the dune

In the top model, foredune was the only explanatory variable (9% variance explained). Third, patterns for total carbon density (aboveground grass, belowground grass, and sand combined) were similar to those for sand carbon density alone. Total carbon was negatively correlated with sand deposition rate ($p = 0.03$, $n = 33$) and backshore slope ($p = 0.04$, $n = 33$), and positively correlated with SCR ($p = 0.01$, $n = 33$) and foredune aspect ratio ($p = 0.12$, $n = 33$; Table 2). In the top model for total carbon density, SCR was the only explanatory variable (19% variance explained). In the next best model, sand deposition rate, backshore slope, and foredune aspect ratio explained 14, 11, and 6% of the variance, respectively (Table 2). Finally, no explanatory variables explained belowground grass carbon density.

Discussion

Contextualizing Dune Carbon Storage in Outer Banks Foredune Ecosystems

We found that sediment organic carbon density values on the Outer Banks were generally much lower than those reported for other dune ecosystems worldwide (see Table 1 for comparisons). For example, depending on island and profile location, sand carbon density measurements were approximately 3–5 times higher in Italian mobile dunes (grass-dominated dunes most comparable to our sites) than in the Outer Banks region (Fig. 5; Table 1; Table S5; Drius et al., 2016). Likewise, measurements reported for grass-dominated UK Atlantic dunes were approximately 6–8 times higher than those in our system (Table 1; Beaumont et al., 2014). However, when compared to dunes on other US Atlantic Coast barrier islands (e.g., Sapelo Island, Georgia; Tackett & Craft, 2010), our system had similar sand percent carbon values, suggesting that sand carbon content is relatively low and may vary little across the region (Table 1; Table S5).

The variation in carbon storage among dunes worldwide is likely a consequence of factors including plant productivity, decomposition rates, and microbial processes, which are shaped by factors such as climate, sand supply, and disturbance from extreme storms (Sevink, 1991). For example, the UK coastal dunes in Beaumont et al. (2014) have much higher aboveground vegetation biomass, averaging 1375 and 1221 g m^{-2} in mobile dunes and fixed dunes, respectively, compared with averages of 100–350 g m^{-2} on the Outer Banks foredunes in this study. The Italian mobile dunes are largely dominated by *A. arenaria* (Drius et al., 2016), which typically grows more densely than *U. paniculata* and may have higher biomass (Hacker et al., 2019). Beyond differences in vegetation and climate among these sites, US Atlantic barrier islands are also highly dynamic systems, subjected to frequent disturbance and overwash from extreme storms, which can erode dunes partially or completely, limiting soil development and vegetation growth (Rossi & Rabenhorst, 2019). For example, a study on French Atlantic dunes found higher decomposition rates associated with greater sand accumulation, but this relationship broke down when disturbance led to the erosion of dunes (Laporte-Fauret et al., 2021).

How do carbon stocks in dunes compare to those in other coastal and grassland ecosystems? On a carbon density basis, dune aboveground carbon stocks (0.004 to 0.19 kg C m^{-2}; Fig. 5; Table S5) were comparable to those in eelgrass meadows, salt marshes, and terrestrial grasslands; for example, aboveground carbon stocks ranged from 0.03 to 2.30 kg C m^{-2} in New England eelgrass meadows (Novak et al., 2020), averaged 0.10 kg C m^{-2} in Florida salt marshes (Dontis et al., 2020), and ranged from 0.05 to 0.60 kg C m^{-2} in grasslands worldwide (e.g., Bradley et al., 2006; Cao & Woodward, 1998; Tanentzap & Coomes, 2012; Xia et al., 2014). Studies on dunes, including ours, show that sediment organic carbon values are substantially lower than those in other coastal and grassland systems. For example, soil carbon stocks in New England (2–6 kg C m^{-2}; Novak et al., 2020) and Pacific Northwest (7–9 kg C m^{-3}; Kauffman et al., 2020) eelgrass meadows and terrestrial grasslands (i.e., 2.5–17.5 kg C m^{-2}; 0.5–8%C; Cao & Woodward, 1998; Conant et al., 2001) were up to 10 times greater than

values in Outer Banks dunes (i.e., 0.25–1.9 kg C m^{-2}; Fig. 5; Table S5). Sediment carbon stocks were even greater in marshes and mangroves, with averages of 10, 46, and 28 kg C m^{-2} in salt marshes, freshwater marshes, and mangroves, respectively (Van Atwood et al., 2017; de Broek et al., 2016). A key factor controlling carbon sequestration in these wetland blue carbon systems is the absence of oxidation, as anaerobic conditions help make carbon stocks more resistant to decay (e.g., McLeod et al., 2011). Unlike wetlands, dunes do not experience daily flooding and typically have higher sediment grain sizes, increasing the oxidation of stored carbon back into CO_2 and decreasing carbon storage.

While sand carbon density values in our study area were low than those in other coastal or grassland ecosystems, dunes are characterized by high sand and plant biomass burial rates (e.g., Hacker et al., 2012) in comparison to these systems. As result, dunes are likely to have much greater sediment volumes, with extensive underground rhizome networks that depend on vertical expansion to keep pace with sand deposition, which can exceed 0.3 m or more per year (Charbonneau et al., 2016; Hacker et al., 2012, 2019). Considering that foredunes can reach heights of 15–20 m or more in certain systems (for example, see Hacker et al., 2012), contain extensive belowground rhizome networks, and have a high proportion of carbon stored in belowground grass stocks (Fig. 4), we expect that total carbon storage in dunes is substantial at sites with high dune volumes.

Patterns in Sand and Belowground Grass Carbon Density with Depth

Surprisingly, we found no apparent differences in sand or belowground grass carbon density with depth (Fig. S6; Table S4; note that more of our samples were between 0 and 60 cm deep within our 1 m cores, with lower sampling density from 60 to 100 cm, see Table S2 for details). We expected that sand carbon density would be highest at the top of the core, where plant roots, rhizomes, and plant litter are most abundant, and decrease with depth as roots and rhizomes decline and/or decompose over time (as shown in other coastal ecosystems; e.g., Kauffman et al., 2020; Stepanek, 2023). Instead, we found that little relationship between sand carbon density and belowground plant carbon density, and both rarely varied with depth; when they did, they peaked in the middle (~ 30–50 cm) or near the bottom (~ 70–100 cm) of the core in some cases (Fig. S6; Table S3). This lack of relationship may be due to the frequent disturbance that these dunes experience (Hovenga et al., 2021), which may remove or deposit large amounts of sand and plant material, likely increasing spatial heterogeneity in organic matter with depth. In addition, sampling to greater depths than 1 m may be necessary to observe declines in carbon with depth.

Factors Important to Foredune Carbon Stocks

We observed spatial variability in carbon stocks along the dune profile and across the Outer Banks barrier islands, likely due to differences in beach and foredune geomorphology and ecology. Overall, aboveground vegetation carbon density increased landward along the dune profile, with the lowest values at the dune toe and the highest at the dune crest and heel (Fig. 5; Table S7). Similarly, sand carbon densities also showed a tendency to increase in the landward direction along the dune profile. Unsurprisingly, belowground grass carbon followed similar patterns to aboveground grass carbon along the dune profile. However, the significantly higher belowground carbon values observed at OCR (Fig. 5B) were an unexpected and may be related to foredune morphology. Dunes at this site were particularly tall and narrow (Fig. 2E), which could have led to a greater density of belowground plant biomass per volume of the dune.

We also observed variability in sand carbon density among the islands, with the highest values in the south (SCB) and the lowest values at BOD (Fig. 5C). We explored whether this spatial variability in sand carbon stocks was correlated with beach and foredune morphology, sand supply, and grass abundance metrics. Overall, we found that sand supply at the core location, or foredune morphometrics influencing sand supply (i.e., backshore slope, foredune height; Fig. 3C, E), were the most important factors contributing to variability in dune carbon stocks (Table 2). For example, both total foredune carbon (including vegetation and sand) and sand carbon stocks were negatively correlated with sand supply to the core location and backshore slope. This finding was somewhat unexpected, as high burial rates are often been associated with high carbon stocks in other coastal ecosystems (e.g., Breithaupt et al., 2019; Callaway et al., 2012; Lovelock et al., 2014). In this system, however, high dune sand supply appears to "dilute" dune carbon with low-carbon-content beach sand, reducing the carbon contribution from dune grasses and effectively lowering sand carbon density. Some of our sites received > 25 cm of sand annually over a 2-year period, with the greatest deposition occurring at BOD, where sand carbon density values were the lowest of our study sites (Figs. 2F, 4C, and 6).

Our analyses allowed us to explore the interactive effects of sand deposition rate, grass density, and biomass on sand carbon density across our study region.

Grass density (all species combined) was included in the top model (using ΔAIC) for sand carbon density, but it explained a small proportion of the variance compared to dune sand deposition rate and backshore slope (4% compared to 50% for dune sand deposition rate and 26% for backshore slope). This finding contradicted our expectation that aboveground vegetation would be one of the most important factors determining sand carbon storage, as has been shown in some other coastal systems (e.g., Greiner et al., 2013; Kaviarasan et al., 2019; Rossi & Rabenhorst, 2019). The lack of a strong relationship between dune grasses and sand carbon stocks could be result from the interaction between sand deposition and dune grass biomass across islands and profile locations. For example, at locations with high sand deposition (for example, at BOD and OCR), dune grass biomass is also elevated, likely to the well-documented positive feedback between sand accretion and vegetative growth in dunes (e.g., Biel et al., 2019; Charbonneau et al., 2021; Hacker et al., 2012; Keijsers et al., 2015; Zarnetske et al., 2012). This positive feedback could indirectly contribute to the "dilution" of sand carbon through increased sand accretion. However, across the dune profile, gradients in sand deposition and grass density are negatively correlated. The dune toe and crest are characterized by high deposition (or erosion) and overall lower grass abundance, while the dune heel exhibits the opposite pattern, with low sand deposition (or erosion) and high grass abundance (Fig. 6). Under these conditions, we found that sand carbon varies from low at the dune toe and crest to high at the heel, where the effect of belowground roots and rhizomes, decomposition, and soil formation is likely greatest (e.g., Miller et al., 2010). Thus, the feedback between dune sand deposition, grass density, and sand carbon density is self-reinforcing at both high and low sand deposition sites. At sites with high vegetation biomass, sand deposition is also high due to positive feedback, which ultimately dilutes sand carbon. Conversely, the profile location with the highest vegetation biomass and lowest sand deposition (foredune heel) shows the highest sand carbon density. This suggests that the role of vegetation to sand carbon stocks is complex and likely depends on its indirect effects on sand deposition and its direct effects on belowground carbon cycling.

Periodic declines in aboveground vegetation density following storm disturbance are also a critical consideration in dynamic foredune ecosystems, as previously shown in mangroves (Breithaupt et al., 2019). Hurricane Florence struck nine months prior to our coring campaign, overwashing and removing much of the toe and crest at two SCB sites (SCB_6 and SCB_9; Fig. 2I, J). These transects exhibited unusually high and similar sand carbon values, likely because they were collected in the previous dune heel profile location, a later successional plant community that had not been eroded away. Therefore, storm events can wash away or redistribute dune carbon stocks by moving large volumes of sediment, disrupting vegetation productivity and succession, and ultimately affecting carbon storage both along the dune profile and with depth.

Our study suggests that carbon stocks in coastal foredunes are linked to geomorphic and vegetation processes, which vary spatially along coastlines. While other studies have made such linkages in coastal ecosystems including mangroves, marshes, and barrier islands (e.g., Callaway et al., 2012; Lovelock et al., 2014; Novak et al., 2020; Rossi & Rabenhorst, 2019; Twilley et al., 2018), our study is one of the first to make such connections in foredunes (also see Stepanek, 2023). For example, Novak et al. (2020) investigated variability in eelgrass carbon stocks and found that sediment grain size, tidal range, shoot density, and wave energy were important factors. In marshes and mangroves, previous studies have shown that carbon sequestration varies according to plant community type, sediment characteristics, and sediment accretion rates (Callaway et al., 2012; Lovelock et al., 2014).

Similar to standing carbon stocks, which we document here, rates of carbon accumulation can also be impacted by dynamic coastal processes. Although we report differences in dune carbon stocks across the Outer Banks, carbon accumulation rates may not follow the same patterns. Therefore, future work characterizing the temporal dynamics of this system may provide key insights into the processes controlling dune carbon storage. For example, Lovelock et al. (2014) reported large differences in sediment carbon density across a gradient of nutrient availability in mangrove forests, but carbon sequestration rates were similar across the same region due to differences in vertical sediment accumulation rates. This suggests that dune sites with low sand carbon density but higher sand deposition (e.g., BOD and OCR, which averaged 0.25–0.32 kg C m^{-3} and 0.41–0.79 kg C m^{-3}, respectively, depending on profile location) could have similar carbon sequestration rates to those dune sites with higher sand carbon density but lower sand deposition (e.g., SCB, which averaged 0.89–1.86 kg C m^{-3}, depending on profile location; Figs. 2 and 4).

Global Change Implications for Dune Ecosystem Services

Human activities and land-use change can lead to increased loss of dunes, shifts in plant communities, disruptions in nutrient cycling (Macreadie et al., 2019). Additionally, sea-level rise and extreme storms can result in inundation and erosion (Enríquez et al., 2019; Fernández-Montblanc et al.,

2020; Seabloom et al., 2013; Stockdon et al., 2007), all of which may interactively affect dune carbon storage. Carbon sequestration rates in dunes may increase if sediment accumulation keeps pace with sea-level rise and dunes are able to migrate landward with erosion. However, this is likely to be accompanied by the redistribution or loss of carbon stocks during periods of erosion and overwash associated with migration. Modeling and field-based empirical efforts have demonstrated that rates of sea-level rise and vegetation growth can determine whether foredunes maintain their volume, migrate landward, or revegetate and recover to their previous height following disturbance (Feagin et al., 2015; Keijsers et al., 2016; van IJzendoorn et al., 2021). Some even suggested that global "greening" of ecosystems is occurring as a result of climate change (Zhu et al., 2016). In coastal dunes, Jackson et al. (2019) found global increases in vegetation cover over the past three decades, driven by the interactive effects of increased temperatures, precipitation, and nutrient availability. These climate change impacts could lead to complicated dynamics for dunes and their carbon storage services.

Dune grass range shifts may also have implications for carbon storage. Goldstein et al. (2018) documented potential range shifts of *U. paniculata* and *A. breviligulata* on the Atlantic coast using literature surveys. They found a northward increase in the range of *U. paniculata* over the past 60 years that may be associated with warming trends observed near the grass species' northern range limit. Previous studies indicate that *U. paniculata* growth and germination are limited by low wintertime temperatures (Godfrey, 1977; Seneca, 1969), preventing it from growing in more northern regions. This suggests that warming in these areas could release it from this range limitation. Combined with glasshouse study findings, where *A. breviligulata* growth declined when grown in a mixture with *U. paniculata* (Harris et al., 2017), there is evidence that *U. paniculata* could outcompete *A. breviligulata* within areas of its range with future warming. Based on our measurements of grass morphology (see Hacker et al., 2019) and field densities of each species in monoculture, we predict an approximately 35% increase in aboveground grass carbon stocks if a dune shift from *A. breviligulata* monoculture to *U. paniculata* monoculture. To determine how shifts in dominant dune vegetation may affect carbon storage ecosystem services, future work should quantify rates of carbon accumulation in dunes and investigate the relationships and feedbacks between vegetation and sand deposition that lead to variable carbon storage.

In this study, we present one of the first comprehensive regional inventories of coastal foredune carbon storage in North America (also see Stepanek, 2023). Our findings enhance the understanding of carbon storage ecosystem services in understudied dune systems and provide insights into the physical and ecological factors that may influence carbon storage in dynamic coastal settings. This improved understanding of dune carbon dynamics can inform efforts to predict future changes in dune carbon stocks due to heightened storm events and sea-level rise, offering insight into the future role of coastal dunes in mitigating climate change.

Supplementary Information The online version contains supplementary material available at https://doi.org/10.1007/s12237-025-01484-6.

Acknowledgements We thank P. Hovenga, R. Mostow, M. Itzkin, E. Mullins, I. Reeves, J. Wood, H. Lawrence, N. Cohn, E. Goldstein, C. Magel, and R. Biel for assistance with field data collection and P. Hovenga for assistance with topography data processing. We are grateful to M. Goni and K. Welch for assistance with obtaining and interpreting sand percent carbon data, A. Fund for grass percent carbon analyses, A. Thurber for use of his laboratory facilities for LOI analyses, and E. Peck for advice on core collection and lab methodology. We thank B. Russell for designing and creating our custom-built core extruder.

Author Contribution All authors contributed to the study's conception and design. Data collection was performed by KRJ, CJH, and JS. Sample and data analyses were conducted by KRJ. The first draft of the manuscript was written by KRJ. All authors contributed to the writing and editing of the final manuscript.

Funding Funding was provided by the National Oceanic and Atmospheric Administration (NOAA) through the NOS/NCCOS/CRP Ecological Effects of Sea Level Rise Program (grant no. NA15NOS4780172) to PR, SDH, and LJM; the Geological Society of America to KRJ; the Garden Club of America to KRJ; the NSF Graduate Research Fellowship Program to CJH; and the ARCS Foundation Fellowship Program to CJH.

Data Availability The field survey data collected as part of this study is available via the Environmental Data Initiative (EDI; Jay et al. 2022b). Dune carbon storage data can be made available upon request.

Declarations

Conflict of Interest The authors declare no conflict of interest.

References

Atwood, T. B., Connolly, R. M., Almahasheer, H., Carnell, P. E., Duarte, C. M., Ewers Lewis, C. J., Irigoien, X., et al. (2017).

Global patterns in mangrove soil carbon stocks and losses. *Nature Climate Change, 7*, 523–528. https://doi.org/10.1038/nclimate3326

Barbier, E. B., Hacker, S. D., Kennedy, C., Koch, E. W., Stier, A. C., & Silliman, B. R. (2011). The value of estuarine and coastal ecosystem services. *Ecological Monographs, 81*, 169–193. https://doi.org/10.1890/10-1510.1

Barreiro, F., Gómez, M., López, J., Lastra, M., & de la Huz, R. (2013). Coupling between macroalgal inputs and nutrients outcrop in exposed sandy beaches. *Hydrobiologia, 700*, 73–84. https://doi.org/10.1007/s10750-012-1220-z

Bauer, B. O., & Davidson-Arnott, R. G. D. (2002). A general framework for modeling sediment supply to coastal dunes including wind angle, beach geometry, and fetch effects. *Geomorphology, 49*, 89–108. https://doi.org/10.1016/S0169-555X(02)00165-4

Beaumont, N. J., Jones, L., Garbutt, A., Hansom, J. D., & Toberman, M. (2014). The value of carbon sequestration and storage in coastal habitats. *Estuarine, Coastal and Shelf Science, 137*, 32–40. https://doi.org/10.1016/j.ecss.2013.11.022

Biel, R. G., Hacker, S. D., & Ruggiero, P. (2019). Elucidating coastal foredune ecomorphodynamics in the U.S. Pacific Northwest via Bayesian Networks. *Journal of Geophysical Research: Earth Surface, 124*, 1919–1938. https://doi.org/10.1029/2018JF004758

Bouillon, S., Dahdouh-Guebas, F., Rao, A. V. V. S., Koedam, N., & Dehairs, F. (2003). Sources of organic carbon in mangrove sediments: Variability and possible ecological implications. *Hydrobiologia, 495*, 7.

Bouillon, Steven, A. V. Borges, E. Castañeda-Moya, K. Diele, T. Dittmar, N. C. Duke, E. Kristensen, et al. (2008). Mangrove production and carbon sinks: a revision of global budget estimates: Global mangrove carbon budgets. *Global Biogeochemical Cycles* 22: GB2013. https://doi.org/10.1029/2007GB003052.

Bradley, B. A., Houghton, R. A., Mustard, J. F., & Hamburg, S. P. (2006). Invasive grass reduces aboveground carbon stocks in shrublands of the Western US. *Global Change Biology, 12*, 1815–1822. https://doi.org/10.1111/j.1365-2486.2006.01232.x

Breithaupt, J. L., Smoak, J. M., Sanders, C. J., & Troxler, T. G. (2019). Spatial variability of organic carbon, CaCO3 and nutrient burial rates spanning a mangrove productivity gradient in the coastal Everglades. *Ecosystems, 22*, 844–858. https://doi.org/10.1007/s10021-018-0306-5

Breithaupt, J. L., J. M. Smoak, T. J. Smith, C. J. Sanders, and A. Hoare. (2012). Organic carbon burial rates in mangrove sediments: Strengthening the global budget. *Global Biogeochemical Cycles* 26: GB3011. https://doi.org/10.1029/2012GB004375.

Brown, J. K., & Zinnert, J. C. (2018). Mechanisms of surviving burial: Dune grass interspecific differences drive resource allocation after sand deposition. *Ecosphere, 9*, e02162. https://doi.org/10.1002/ecs2.2162

Bryant, M. A., Hesser, T. J., & Jensen, R. E. (2016). *Evaluation statistics computed for the Wave Information Studies (WIS)*. ERDC/CHL-CHETN-I-91. U.S. Army Engineer Research and Development Center.

Callaway, J. C., Borgnis, E. L., Turner, R. E., & Milan, C. S. (2012). Carbon sequestration and sediment accretion in San Francisco Bay tidal wetlands. *Estuaries and Coasts, 35*, 1163–1181. https://doi.org/10.1007/s12237-012-9508-9

Cao, M., & Woodward, F. I. (1998). Net primary and ecosystem production and carbon stocks of terrestrial ecosystems and their responses to climate change. *Global Change Biology, 4*, 185–198. https://doi.org/10.1046/j.1365-2486.1998.00125.x

Charbonneau, B. R., Wnek, J. P., Langley, J. A., Lee, G., & Balsamo, R. A. (2016). Above vs. belowground plant biomass along a barrier island: Implications for dune stabilization. *Journal of Environmental Management, 182*, 126–133. https://doi.org/10.1016/j.jenvman.2016.06.032

Charbonneau, B. R., Dohner, S. M., Wnek, J. P., Barber, D., Zarnetske, P., & Casper, B. B. (2021). Vegetation effects on coastal foredune initiation: Wind tunnel experiments and field validation for three dune-building plants. *Geomorphology, 378*, 107594. https://doi.org/10.1016/j.geomorph.2021.107594

Chen, C. R., Hou, E. Q., Condron, L. M., Bacon, G., Esfandbod, M., Olley, J., & Turner, B. L. (2015). Soil phosphorus fractionation and nutrient dynamics along the Cooloola coastal dune chronosequence, southern Queensland, Australia. *Geoderma, 257–258*, 4–13. https://doi.org/10.1016/j.geoderma.2015.04.027

Chmura, G. L., S. C. Anisfeld, D. R. Cahoon, and J. C. Lynch. (2003). Global carbon sequestration in tidal, saline wetland soils. *Global Biogeochemical Cycles* 17. https://doi.org/10.1029/2002GB001917.

Cohn, N., Hoonhout, B., Goldstein, E., De Vries, S., Moore, L., Durán-Vinent, O., & Ruggiero, P. (2019). Exploring marine and aeolian controls on coastal foredune growth using a coupled numerical model. *Journal of Marine Science and Engineering, 7*, 13. https://doi.org/10.3390/jmse7010013

Conant, R. T., Paustian, K., & Elliott, E. T. (2001). Grassland management and conversion into grassland: Effects on soil carbon. *Ecological Applications, 11*, 343–355. https://doi.org/10.1890/1051-0761(2001)011[0343:GMACIG]2.0.CO;2

Dean, Jr. (1974). Determination of carbonate and organic matter in calcareous sediments and sedimentary rocks by loss on ignition: Comparison with other methods. *SEPM Journal of Sedimentary Research, 44*, 242–248. https://doi.org/10.1306/74D729D2-2B21-11D7-8648000102C1865D

Donato, D. C., Kauffman, J. B., Murdiyarso, D., Kurnianto, S., Stidham, M., & Kanninen, M. (2011). Mangroves among the most carbon-rich forests in the tropics. *Nature Geoscience, 4*, 293–297. https://doi.org/10.1038/ngeo1123

Dontis, E. E., Radabaugh, K. R., Chappel, A. R., Russo, C. E., & Moyer, R. P. (2020). Carbon storage increases with site age as created salt marshes transition to mangrove forests in Tampa Bay, Florida (USA). *Estuaries and Coasts, 43*, 1470–1488. https://doi.org/10.1007/s12237-020-00733-0

Drius, M., Carranza, M. L., Stanisci, A., & Jones, L. (2016). The role of Italian coastal dunes as carbon sinks and diversity sources. *A Multi-Service Perspective. Applied Geography, 75*, 127–136. https://doi.org/10.1016/j.apgeog.2016.08.007

Duarte, C. M. (2017). Reviews and syntheses: Hidden forests, the role of vegetated coastal habitats in the ocean carbon budget. *Biogeosciences, 14*, 301–310. https://doi.org/10.5194/bg-14-301-2017

Duarte, C. M., N. Marbà, E. Gacia, J. W. Fourqurean, J. Beggins, C. Barrón, and E. T. Apostolaki. (2010). Seagrass community metabolism: assessing the carbon sink capacity of seagrass meadows. *Global Biogeochemical Cycles* 24: GB4032. https://doi.org/10.1029/2010GB003793.

Dugan, J. E., Hubbard, D. M., Page, H. M., & Schimel, J. P. (2011). Marine macrophyte wrack inputs and dissolved nutrients in beach sands. *Estuaries and Coasts, 34*, 839–850. https://doi.org/10.1007/s12237-011-9375-9

Duran, O., & Moore, L. J. (2013). Vegetation controls on the maximum size of coastal dunes. *Proceedings of the National Academy of Sciences, 110*, 17217–17222. https://doi.org/10.1073/pnas.1307580110

Enríquez, A. R., Marcos, M., Falqués, A., & Roelvink, D. (2019). Assessing beach and dune erosion and vulnerability under sea level rise: A case study in the Mediterranean Sea. *Frontiers in Marine Science, 6*, 4. https://doi.org/10.3389/fmars.2019.00004

Feagin, R. A., Figlus, J., Zinnert, J. C., Sigren, J., Martínez, M. L., Silva, R., Smith, W. K., Cox, D., Young, D. R., & Carter, G. (2015). Going with the flow or against the grain? The promise of

vegetation for protecting beaches, dunes, and barrier islands from erosion. *Frontiers in Ecology and the Environment, 13*, 203–210. https://doi.org/10.1890/140218

Fernández-Montblanc, T., Duo, E., & Ciavola, P. (2020). Dune reconstruction and revegetation as a potential measure to decrease coastal erosion and flooding under extreme storm conditions. *Ocean & Coastal Management, 188*, 105075. https://doi.org/10.1016/j.ocecoaman.2019.105075

Fox, J., M. Friendly, and G. Monette. 2018. heplots: visualizing tests in multivariate linear models. (version R package version 1.3–5.). https://CRAN.R-project.org/package=heplots.

Godfrey, P. J. (1977). Climate, plant response and development of dunes on barrier beaches along the U.S. East Coast. *International Journal of Biometeorology, 21*, 203–215.

Godfrey, P. J., & Godfrey, M. M. (1973). Comparison of geological and geomorphic interactions between altered and unaltered barrier island systems in North Carolina. In D. R. Coates (Ed.), *Coastal Geomorphology* (pp. 239–258). State Univeristy of New York.

Goldstein, E. B., Moore, L. J., & DuránVinent, O. (2017). Lateral vegetation growth rates exert control on coastal foredune hummockiness and coalescing time. *Earth Surface Dynamics, 5*, 417–427. https://doi.org/10.5194/esurf-5-417-2017

Goldstein, E. B., E. V. Mullins, L. J. Moore, R. G. Biel, J. K. Brown, S. D. Hacker, K. R. Jay, R. S. Mostow, P. Ruggiero, and J. C. Zinnert. (2018). Literature-based latitudinal distribution and possible range shifts of two US east coast dune grass species (*Uniola paniculata* and *Ammophila breviligulata*). *PeerJ* 6. PeerJ Inc.: e4932. https://doi.org/10.7717/peerj.4932.

Greiner, J. T., K. J. McGlathery, J. Gunnell, and B. A. McKee. (2013). Seagrass restoration enhances "blue carbon" sequestration in coastal waters. *PLOS ONE* 8. Public Library of Science: e72469. https://doi.org/10.1371/journal.pone.0072469.

Hacker, S. D., Zarnetske, P., Seabloom, E., Ruggiero, P., Mull, J., Gerrity, S., & Jones, C. (2012). Subtle differences in two non-native congeneric beach grasses significantly affect their colonization, spread, and impact. *Oikos, 121*, 138–148. https://doi.org/10.1111/j.1600-0706.2011.18887.x

Hacker, S. D., Jay, K. R., Cohn, N., Goldstein, E. B., Hovenga, P. A., Itzkin, M., Moore, L. J., Mostow, R. S., Mullins, E. V., & Ruggiero, P. (2019). Species-specific functional morphology of four US Atlantic Coast dune grasses: Biogeographic implications for dune shape and coastal protection. *Diversity, 11*, 1–16. https://doi.org/10.3390/d11050082

Harris, A. L., Zinnert, J. C., & Young, D. R. (2017). Differential response of barrier island dune grasses to species interactions and burial. *Plant Ecology, 218*, 609–619. https://doi.org/10.1007/s11258-017-0715-0

Heiri, O., Lotter, A. F., & Lemcke, G. (2001). *Loss on Ignition as a Method for Estimating Organic and Carbonate Content in Sediments: Reproducibility and Comparability of Results, 25*, 101–110.

Hesp, P. (2002). Foredunes and blowouts: Initiation, geomorphology and dynamics. *Geomorphology, 48*, 245–268. https://doi.org/10.1016/S0169-555X(02)00184-8

Hesp, P. A., & Walker, I. J. (2013). Aeolian environments: Coastal dunes. In J. Shroder, N. Lancaster, D. J. Sherman, & A. C. W. Baas (Eds.), *Treatise on Geomorphology* (vol 11). Academic Press, pp 109–133.

Hesp, Patrick A. (1989). A review of biological and geomorphological processes involved in the initiation and development of incipient foredunes. *Proceedings of the Royal Society of Edinburgh, Section B: Biological Sciences* 96. Royal Society of Edinburgh Scotland Foundation: 181–201. https://doi.org/10.1017/S0269727000010927.

Hopkinson, C. S., Cai, W.-J., & Hu, X. (2012). Carbon sequestration in wetland dominated coastal systems—a global sink of rapidly diminishing magnitude. *Current Opinion in Environmental Sustainability, 4*, 186–194. https://doi.org/10.1016/j.cosust.2012.03.005

Hovenga, P. A., P. Ruggiero, N. Cohn, K. R. Jay, S. D. Hacker, M. Itzkin, and L. Moore. (2019). Drivers of dune evolution in Cape Lookout National Seashore, NC. In *Coastal Sediments 2019*, 1283–1296. Tampa/St. Petersburg, Florida, USA: World Scientific. https://doi.org/10.1142/9789811204487_0112.

Hovenga, P. A., P. Ruggiero, E. B. Goldstein, S. D. Hacker, and L. J. Moore. (2021). The relative role of constructive and destructive processes in dune evolution on Cape Lookout National Seashore, North Carolina, USA. *Earth Surface Processes and Landforms*: esp.5210. https://doi.org/10.1002/esp.5210.

Howard, J., Sutton-Grier, A., Herr, D., Kleypas, J., Landis, E., Mcleod, E., Pidgeon, E., & Simpson, S. (2017). Clarifying the role of coastal and marine systems in climate mitigation. *Frontiers in Ecology and the Environment, 15*, 42–50. https://doi.org/10.1002/fee.1451

Intergovernmental Panel on Climate Change. (2014). *Climate change 2014: Impacts, adaptation, and vulnerability: Working Group II contribution to the fifth assessment report of the Intergovernmental Panel on Climate Change*. Edited by Christopher B. Field and Vicente R. Barros. Cambridge University Press.

Jackson, D. W. T., Costas, S., González-Villanueva, R., & Cooper, A. (2019). A global 'greening' of coastal dunes: An integrated consequence of climate change? *Global and Planetary Change, 182*, 103026. https://doi.org/10.1016/j.gloplacha.2019.103026

Jay, K. R., Hacker, S. D., Hovenga, P. A., Moore, L. J., & Ruggiero, P. (2022a). Sand supply and dune grass species density affect foredune shape along the US Central Atlantic Coast. *Ecosphere, 13*, e4256. https://doi.org/10.1002/ecs2.4256

Jay, K. R., Hacker, S. D., Hovenga, P. A., Moore, L. J., Ruggiero, P., Itzkin, M., Mostow, R., et al. (2022b). Surveys of coastal foredune topography and vegetation abundance, U.S. North Carolina Outer Banks, 2016-2018. *Environmental Data Initiative*. https://doi.org/10.6073/PASTA/59770602BA34230815F31F55DA5C61E5

Jones, M. B., & Donnelly, A. (2004). Carbon sequestration in temperate grassland ecosystems and the influence of management, climate and elevated CO_2. *New Phytologist, 164*, 423–439. https://doi.org/10.1111/j.1469-8137.2004.01201.x

Jones, M. L. M., Sowerby, A., Williams, D. L., & Jones, R. E. (2008). Factors controlling soil development in sand dunes: Evidence from a coastal dune soil chronosequence. *Plant and Soil, 307*, 219–234. https://doi.org/10.1007/s11104-008-9601-9

Kauffman, J. B., Giovanonni, L., Kelly, J., Dunstan, N., Borde, A., Diefenderfer, H., Cornu, C., Janousek, C., Apple, J., & Brophy, L. (2020). Total ecosystem carbon stocks at the marine-terrestrial interface: Blue carbon of the Pacific Northwest Coast, United States. *Global Change Biology, 26*, 5679–5692. https://doi.org/10.1111/gcb.15248

Kaviarasan, T., Dahms, H. U., Gokul, M. S., Henciya, S., Muthukumar, K., Shankar, S., & Arthur James, R. (2019). Seasonal species variation of sediment organic carbon stocks in salt marshes of Tuticorin Area, southern India. *Wetlands, 39*, 483–494. https://doi.org/10.1007/s13157-018-1094-6

Keijsers, J. G. S., De Groot, A. V., & Riksen, M. J. P. M. (2015). Vegetation and sedimentation on coastal foredunes. *Geomorphology, 228*, 723–734. https://doi.org/10.1016/j.geomorph.2014.10.027

Keijsers, J. G. S., De Groot, A. V., & Riksen, M. J. P. M. (2016). Modeling the biogeomorphic evolution of coastal dunes in response to climate change. *Journal of Geophysical Research: Earth Surface, 121*, 1161–1181. https://doi.org/10.1002/2015JF003815

Kennedy, H., J. Beggins, C. M. Duarte, J. W. Fourqurean, M. Holmer, N. Marbà, and J. J. Middelburg. (2010). Seagrass sediments as a global carbon sink: isotopic constraints. *Global Biogeochemical Cycles* 24: GB4026. https://doi.org/10.1029/2010GB003848.

Kratzmann, M. G., Himmelstoss, E. A., & Thieler, E. R. (2017). *National assessment of shoreline change – A GIS compilation of updated vector shorelines and associated shoreline change data for the Southeast Atlantic Coast*. 2017–1015. Data Release. U.S. Geological Survey.

Kristensen, E., Bouillon, S., Dittmar, T., & Marchand, C. (2008). Organic carbon dynamics in mangrove ecosystems: A review. *Aquatic Botany, 89*, 201–219. https://doi.org/10.1016/j.aquabot.2007.12.005

Lal, R. (2005). Forest soils and carbon sequestration. *Forest Ecology and Management, 220*, 242–258. https://doi.org/10.1016/j.foreco.2005.08.015

Lal, R., Smith, P., Jungkunst, H. F., Mitsch, W. J., Lehmann, J., Nair, P. K. R., McBratney, A. B., et al. (2018). The carbon sequestration potential of terrestrial ecosystems. *Journal of Soil and Water Conservation, 73*, 145A-152A. https://doi.org/10.2489/jswc.73.6.145A

Laporte-Fauret, Q., Alonso Ayuso, A. T., Rodolfo-Damiano, T., Marieu, V., Castelle, B., Bujan, S., Rosebery, D., & Michalet, R. (2021). The role of physical disturbance for litter decomposition and nutrient cycling in coastal sand dunes. *Ecological Engineering, 162*, 106181. https://doi.org/10.1016/j.ecoleng.2021.106181

Lazarus, E. D., & Murray, A. B. (2011). An integrated hypothesis for regional patterns of shoreline change along the Northern North Carolina Outer Banks, USA. *Marine Geology, 281*, 85–90. https://doi.org/10.1016/j.margeo.2011.02.002

Lovelock, C. E., Adame, M. F., Bennion, V., Hayes, M., O'Mara, J., Reef, R., & Santini, N. S. (2014). Contemporary rates of carbon sequestration through vertical accretion of sediments in mangrove forests and saltmarshes of south east Queensland, Australia. *Estuaries and Coasts, 37*, 763–771. https://doi.org/10.1007/s12237-013-9702-4

Luijendijk, A., Hagenaars, G., Ranasinghe, R., Baart, F., Donchyts, G., & Aarninkhof, S. (2018). The state of the world's beaches. *Scientific Reports, 8*, 6641. https://doi.org/10.1038/s41598-018-24630-6

Luyssaert, S., Schulze, E.-D., Börner, A., Knohl, A., Hessenmöller, D., Law, B. E., Ciais, P., & Grace, J. (2008). Old-growth forests as global carbon sinks. *Nature, 455*, 213–215. https://doi.org/10.1038/nature07276

Macreadie, P. I., Anton, A., Raven, J. A., Beaumont, N., Connolly, R. M., Friess, D. A., Kelleway, J. J., et al. (2019). The future of blue carbon science. *Nature Communications, 10*, 3998. https://doi.org/10.1038/s41467-019-11693-w

Mcleod, E., Chmura, G. L., Bouillon, S., Salm, R., Björk, M., Duarte, C. M., Lovelock, C. E., Schlesinger, W. H., & Silliman, B. R. (2011). A blueprint for blue carbon: Toward an improved understanding of the role of vegetated coastal habitats in sequestering CO_2. *Frontiers in Ecology and the Environment, 9*, 552–560. https://doi.org/10.1890/110004

Middelburg, J. J., Nieuwenhuize, J., Lubberts, R. K., & van de Plassche, O. (1997). Organic carbon isotope systematics of coastal marshes. *Estuarine, Coastal and Shelf Science, 45*, 681–687. https://doi.org/10.1006/ecss.1997.0247

Middleton, B. A., & McKee, K. L. (2001). Degradation of mangrove tissues and implications for peat formation in Belizean island forests. *Journal of Ecology, 89*, 818–828. https://doi.org/10.1046/j.0022-0477.2001.00602.x

Miller, T. E., Gornish, E. S., & Buckley, H. L. (2010). Climate and coastal dune vegetation: Disturbance, recovery, and succession. *Plant Ecology, 206*, 97–104. https://doi.org/10.1007/s11258-009-9626-z

Moore, L. J., Vinent, O. D., & Ruggiero, P. (2016). Vegetation control allows autocyclic formation of multiple dunes on prograding coasts. *Geology, 44*, 559–562. https://doi.org/10.1130/G37778.1

Mull, J., & Ruggiero, P. (2014). Estimating storm-induced dune erosion and overtopping along U.S. West Coast beaches. *Journal of Coastal Research, 298*, 1173–1187. https://doi.org/10.2112/JCOASTRES-D-13-00178.1

Mullins, E., Moore, L. J., Goldstein, E. B., Jass, T., Bruno, J., & Vinent, O. D. (2019). Investigating dune-building feedback at the plant level: Insights from a multispecies field experiment. *Earth Surface Processes and Landforms, 44*, 1734–1747. https://doi.org/10.1002/esp.4607

Nellemann, C., Corcoran E., Duarte C. M., Valdés L., De Young C., Fonseca L., & Grimsditch G. (Eds.) (2009). *Blue carbon: The role of healthy oceans in binding carbon: A rapid response assessment*. GRID-Arendal.

Novak, A. B., Pelletier, M. C., Colarusso, P., Simpson, J., Gutierrez, M. N., Arias-Ortiz, A., Charpentier, M., Masque, P., & Vella, P. (2020). Factors influencing carbon stocks and accumulation rates in eelgrass meadows across New England, USA. *Estuaries and Coasts, 43*, 2076–2091. https://doi.org/10.1007/s12237-020-00754-9

Olff, H., Huisman, J., & Tooren, B. F. V. (1993). Species dynamics and nutrient accumulation during early primary succession in coastal sand dunes. *The Journal of Ecology, 81*, 693–706. https://doi.org/10.2307/2261667

Paerl, H. W., N. S. Hall, A. G. Hounshell, R. A. Luettich, K. L. Rossignol, C. L. Osburn, and J. Bales. (2019). Recent increase in catastrophic tropical cyclone flooding in coastal North Carolina, USA: Long-term observations suggest a regime shift. *Scientific Reports* 9. Nature Publishing Group: 10620. https://doi.org/10.1038/s41598-019-46928-9.

Potter, C. (2003). Continental-scale comparisons of terrestrial carbon sinks estimated from satellite data and ecosystem modeling 1982–1998. *Global and Planetary Change, 39*, 201–213. https://doi.org/10.1016/j.gloplacha.2003.07.001

R Development Core Team. (2019). R: a language and environment for statistical computing. Vienna, Austria. www.r-project.org: R Foundation for Statistical Computing.

Reay, D. S., Dentener, F., Smith, P., Grace, J., & Feely, R. A. (2008). Global nitrogen deposition and carbon sinks. *Nature Geoscience, 1*, 430–437. https://doi.org/10.1038/ngeo230

Rossi, A. M., & Rabenhorst, M. C. (2019). Organic carbon dynamics in soils of Mid-Atlantic barrier island landscapes. *Geoderma, 337*, 1278–1290. https://doi.org/10.1016/j.geoderma.2018.10.028

Ruggiero, P., Kaminsky, G. M., Gelfenbaum, G., & Cohn, N. (2016). Morphodynamics of prograding beaches: A synthesis of seasonal- to century-scale observations of the Columbia River littoral cell. *Marine Geology, 376*, 51–68. https://doi.org/10.1016/j.margeo.2016.03.012

Sallenger, A. H., K. S. Doran, and P. A. Howd. (2012). Hotspot of accelerated sea-level rise on the Atlantic coast of North America. *Nature Climate Change* 2. Nature Publishing Group: 884–888. https://doi.org/10.1038/nclimate1597.

Sarmiento, J. L., and N. Gruber. (2002). Sinks for anthropogenic carbon. *Physics Today* 55. American Institute of Physics: 30–36. https://doi.org/10.1063/1.1510279.

Schaub, I., Baum C., Schumann R., & Karsten U. (2019). Effects of an early successional biological soil crust from a temperate coastal sand dune (NE Germany) on soil elemental stoichiometry and phosphatase activity. *Microbial Ecology, 77*, 217–229. https://doi.org/10.1007/s00248-018-1220-2

Seabloom, E. W., Ruggiero, P., Hacker, S. D., Mull, J., & Zarnetske, P. (2013). Invasive grasses, climate change, and exposure to storm-wave overtopping in coastal dune ecosystems. *Global Change Biology, 19*, 824–832. https://doi.org/10.1111/gcb.12078

Seneca, E. D. (1969). Germination response to temperature and salinity of four dune grasses from the Outer Banks of North Carolina. *Ecology, 50*, 45–53. https://doi.org/10.2307/1934661

Sevink, J. (1991). Soil development in the coastal dunes and its relation to climate. *Landscape Ecology, 6*, 49–56. https://doi.org/10.1007/BF00157744

Sherman, D. J., and B. O. Bauer. (1993). Dynamics of beach-dune systems. *Progress in Physical Geography: Earth and Environment* 17. SAGE Publications Ltd: 413–447. https://doi.org/10.1177/030913339301700402.

Short, A. D., & Hesp, P. A. (1982). Wave, beach and dune interactions in southeastern Australia. *Marine Geology, 48*, 259–284. https://doi.org/10.1016/0025-3227(82)90100-1

Stepanek, J. (2023). Carbon storage in U.S. Pacific Northwest coastal dunes: The role of invasive beachgrasses and sand supply. MS Thesis: Oregon State University.

Stockdon, H. F., Sallenger, A. H., Holman, R. A., & Howd, P. A. (2007). A simple model for the spatially-variable coastal response to hurricanes. *Marine Geology, 238*, 1–20. https://doi.org/10.1016/j.margeo.2006.11.004

Tackett, N. W., & Craft, C. B. (2010). Ecosystem development on a coastal barrier island dune chronosequence. *Journal of Coastal Research, 264*, 736–742. https://doi.org/10.2112/08-1167.1

Tanentzap, A. J., & Coomes, D. A. (2012). Carbon storage in terrestrial ecosystems: Do browsing and grazing herbivores matter? *Biological Reviews, 87*, 72–94. https://doi.org/10.1111/j.1469-185X.2011.00185.x

Turner, B. L., & Laliberté, E. (2015). Soil development and nutrient availability along a 2 million-year coastal dune chronosequence under species-rich mediterranean shrubland in southwestern Australia. *Ecosystems, 18*, 287–309. https://doi.org/10.1007/s10021-014-9830-0

Twilley, R. R., Rovai, A. S., & Riul, P. (2018). Coastal morphology explains global blue carbon distributions. *Frontiers in Ecology and the Environment, 16*, 503–508. https://doi.org/10.1002/fee.1937

Underwood, A. J. (1997). *Experiments in ecology: Their logical design and interpretation using analysis of variance*. Cambridge University Press.

Van de Broek, M., Temmerman, S., Merckx, R., & Govers, G. (2016). Controls on soil organic carbon stocks in tidal marshes along an estuarine salinity gradient. *Biogeosciences, 13*, 6611–6624. https://doi.org/10.5194/bg-13-6611-2016

Van der Valk, A. G. (1975). The floristic composition and structure of foredune plant communities of Cape Hatteras National Seashore. *Chesapeake Science, 16*, 115–126.

van IJzendoorn, C. O., S. de Vries, C. Hallin, and P. A. Hesp. (2021). Sea level rise outpaced by vertical dune toe translation on prograding coasts. *Scientific Reports* 11: 12792https://doi.org/10.1038/s41598-021-92150-x

Woodhouse, W. W., Seneca, E. D., & Broome, S. W. (1977). Effect of species on dune grass growth. *International Journal of Biometeorology, 21*, 256–266. https://doi.org/10.1007/BF01552879

Woolard, J. W., & Colby, J. D. (2002). Spatial characterization, resolution, and volumetric change of coastal dunes using airborne LIDAR: Cape Hatteras, North Carolina. *Geomorphology, 48*, 269–287. https://doi.org/10.1016/S0169-555X(02)00185-X

Xia, J., Liu, S., Liang, S., Chen, Y., Xu, W., & Yuan, W. (2014). Spatio-temporal patterns and climate variables controlling of biomass carbon stock of global grassland ecosystems from 1982 to 2006. *Remote Sensing, 6*, 1783–1802. https://doi.org/10.3390/rs6031783

Zarnetske, P. L., Hacker, S. D., Seabloom, E. W., Ruggiero, P., Killian, J. R., Maddux, T. B., & Cox, D. (2012). Biophysical feedback mediates effects of invasive grasses on coastal dune shape. *Ecology, 93*, 1439–1450. https://doi.org/10.1890/11-1112.1

Zarnetske, P. L., Ruggiero, P., Seabloom, E. W., & Hacker, S. D. (2015). Coastal foredune evolution: The relative influence of vegetation and sand supply in the US Pacific Northwest. *Journal of the Royal Society Interface, 12*, 20150017. https://doi.org/10.1098/rsif.2015.0017

Zhu, Z., Piao, S., Myneni, R. B., Huang, M., Zeng, Z., Canadell, J. G., Ciais, P., et al. (2016). Greening of the Earth and its drivers. *Nature Climate Change, 6*, 791–795. https://doi.org/10.1038/nclimate3004